

# BRG1 interacts with SOX10 to establish the melanocyte lineage and to promote differentiation

Himangi G. Marathe<sup>1</sup>, Dawn E. Watkins-Chow<sup>2</sup>, Matthias Weider<sup>3</sup>, Alana Hoffmann<sup>3</sup>, Gaurav Mehta<sup>1</sup>, Archit Trivedi<sup>1</sup>, Shweta Aras<sup>1</sup>, Tupa Basuroy<sup>1</sup>, Aanchal Mehrotra<sup>1</sup>, Dorothy C. Bennett<sup>4</sup>, Michael Wegner<sup>3</sup>, William J. Pavan<sup>2</sup> and Ivana L. de la Serna<sup>1,\*</sup>

<sup>1</sup>Department of Biochemistry and Cancer Biology, University of Toledo College of Medicine and Life Sciences, 3035 Arlington Ave, Toledo, OH 43614, USA, <sup>2</sup>National Human Genome Research Institute, National Institutes of Health, Bethesda, MD 20892-4472, USA, <sup>3</sup>Institut für Biochemie, Emil-Fischer-Zentrum, Friedrich-Alexander Universität Erlangen-Nürnberg, 91054 Erlangen, Germany and <sup>4</sup>Molecular and Clinical Sciences Research Institute, St George's, University of London, London SW17 0RE, UK

Received March 10, 2016; Revised March 10, 2017; Editorial Decision April 03, 2017; Accepted April 04, 2017

## ABSTRACT

**Mutations in *SOX10* cause neurocristopathies which display varying degrees of hypopigmentation. Using a sensitized mutagenesis screen, we identified *Smarca4* as a modifier gene that exacerbates the phenotypic severity of *Sox10* haplo-insufficient mice. Conditional deletion of *Smarca4* in *SOX10* expressing cells resulted in reduced numbers of cranial and ventral trunk melanoblasts. To define the requirement for the *Smarca4*-encoded BRG1 subunit of the SWI/SNF chromatin remodeling complex, we employed *in vitro* models of melanocyte differentiation in which induction of melanocyte-specific gene expression is closely linked to chromatin alterations. We found that BRG1 was required for expression of *Dct*, *Tyrp1* and *Tyr*, genes that are regulated by SOX10 and MITF and for chromatin remodeling at distal and proximal regulatory sites. SOX10 was found to physically interact with BRG1 in differentiating melanocytes and binding of SOX10 to the *Tyrp1* distal enhancer temporally coincided with recruitment of BRG1. Our data show that SOX10 cooperates with MITF to facilitate BRG1 binding to distal enhancers of melanocyte-specific genes. Thus, BRG1 is a SOX10 co-activator, required to establish the melanocyte lineage and promote expression of genes important for melanocyte function.**

## INTRODUCTION

Neurocristopathies are a diverse set of genetic disorders that involve defects in cells derived from the embryonic neural crest (1). Waardenburg syndrome (WS) is a type of neu-

rocristopathy primarily caused by melanocyte deficiencies and manifested by varying degrees of skin and hair hypopigmentation, pigmentation defects of the choroid and iris, and deafness from loss of inner ear melanocytes. There are four clinically distinct WS types that are due to mutations in different genes (2–6): WS1 and WS3 result from mutations in the *PAX3* gene, some cases of WS2 are due to mutations in the Microphthalmia-associated transcription factor (*MITF*) gene and some cases of WS2 and WS4 are due to haploinsufficiency of *SOX10*, which can also result in aganglionosis of the distal colon, and peripheral neuropathies. Individuals with *SOX10* haploinsufficiency display phenotypic variability, suggesting the existence of additional modifier genes.

*SOX10* is a member of the SOX (Sry-related high-mobility-group box) family of transcription factors that is essential for neural crest stem cell survival and for differentiation into melanocytes and Schwann cells (7). Members of this family generally cooperate with other transcriptional regulators to synergistically activate transcription, binding to AT-rich motifs in the minor groove of DNA (8). During Schwann cell differentiation, *SOX10* interacts with a different set of transcription factors to activate genes required for myelination (9–13). *SOX10* has been shown to interact with the SWI/SNF chromatin remodeling complex and to recruit the complex to Schwann cell-specific loci (14,15).

SWI/SNF chromatin remodeling enzymes utilize energy from ATP hydrolysis to physically remodel chromatin and regulate gene expression (16). At the core of the complex is either of two ATPases, BRG1 or BRM, which are encoded by the *Smarca4* and *Smarca2* genes, respectively. BRG1 and BRM each have a conserved ATPase domain that utilizes the energy from ATP hydrolysis to alter DNA-histone interactions, rendering sites accessible to factor binding and in some cases promoting nucleosome repositioning or eviction (17–19). Distinct SWI/SNF complexes containing BRG1

\*To whom correspondence should be addressed. Tel: +1 419 383 4111; Fax: +1 419 383 6228; Email: ivana.delaserna@utoledo.edu

or BRM are formed through associations with 9–11 additional subunits known as BRG1/BRM-associated factors (BAFs) (20). SWI/SNF enzymes lack sequence specificity and are thought to be recruited to target regions primarily by interactions with major transcriptional regulators such as C/EBP factors in myeloid cells and adipocytes (21–23), MYOD in muscle (24,25), NEUROD in neurons (26), SOX10 in Schwann cells (14,15) and MITF in melanocytes (27–29). SWI/SNF enzymes play essential roles in maintaining embryonic pluripotency as well as promoting lineage specification and differentiation (30). Disruption of *Smarca4* causes early embryonic lethality (31). Mice with melanocyte-specific disruption of *Smarca4* fail to develop melanocytes and thus lack pigmentation (29). Schwann cell-specific disruption of *Smarca4* severely compromises Schwann cell differentiation and causes peripheral neuropathy (14). Thus, *Smarca4*-encoded BRG1 is critically required for the development of two neural crest cell-derived lineages, which are both also highly dependent on SOX10. It has been well established that BRG1 interacts with MITF and co-activates MITF target genes in melanocytes and melanoma cells. BRG1 is a SOX10 co-activator in Schwann cells, however it remains to be determined if BRG1 also interacts with SOX10 to regulate melanocyte development and function.

In this study, we employed a previously established N-ethyl-N-nitrosourea (ENU) mutagenesis screen and identified *Smarca4* as a modifier gene that exacerbates the phenotypic severity of *SOX10<sup>LacZ/+</sup>* mice (32). We confirmed that the *Smarca4* mutation was responsible for the pigmentation phenotype by deleting *Smarca4* in SOX10-expressing cells. To mechanistically define the functional interaction between SOX10 and BRG1 in the regulation of genes that promote melanocyte function, we utilized *in vitro* models of melanocyte differentiation and characterized chromatin structural changes at the regulatory regions of melanocyte-specific genes that are induced during differentiation. We found that BRG1 is required for melanocyte differentiation, expression of melanocyte-specific genes, and chromatin remodeling at regulatory sites on SOX10 and MITF target genes. SOX10 was found to interact with BRG1 and to cooperate with MITF in recruiting BRG1 to melanocyte-specific regulatory regions.

## MATERIALS AND METHODS

### Mouse genetics and husbandry

Maintenance of the *Sox10<sup>LacZ</sup>* line (*SOX10<sup>tm1Weg</sup>*) was performed as previously described (32). *SOX10<sup>LacZ</sup>* and *Smarca4<sup>Mos6</sup>* mice were bred and housed in an NHGRI animal facility according to NIH guidelines. Animal care was done in accordance with NHGRI institutional standards and was approved by the Institutional Animal Care and Use Committee, NHGRI, and NIH Institutional Review Board. Mice carrying the Tg(SOX10-cre)<sup>1Wdr</sup> transgene (33) and a floxed BRG1 allele, *Smarca4<sup>tm1.2Pcn</sup>* (34) were bred in the Erlangen animal facility in accord with EU animal welfare laws with approval of the responsible local committees and government bodies.

### Mapping and exome sequencing of the *Smarca4<sup>Mos6</sup>* mutation

A low density genome scan was completed with seven affected mice using 61 SSLP markers (a subset of MIT markers described in (35) polymorphic between the founder strains C57BL/6J and BALBcJ). Because of a mixed genetic background of the founder mouse, a portion of the genome was not informative in this initial mapping. Following this preliminary genome scan, 11 regions were identified as ‘potentially linked’ (two regions of linkage plus an additional nine uninformative regions). One sample from an affected mouse was used for exome sequencing. Sequence variants were filtered to remove low quality variants, variants not predicted to alter coding sequences, variants present in dbSNP, and variants previously identified in other exome sequencing projects of independent mutants on the same genetic background within our laboratory. After filtering, 69 variants remained within the 11 regions of ‘potential linkage’. These variants included two on Chr 9, both within *Smarca4*. Subsequent breeding confirmed segregation of the *Smarca4* variants with the *Mos6* phenotype in 42 mice across three generations.

### Genotyping

The Taqman assay or RT-PCR was used for genotyping.

### *In situ* hybridization, immunohistochemistry and $\beta$ -galactosidase staining

Whole mount *in situ* hybridization was performed essentially as described (36). Embryos underwent overnight fixation in 4% paraformaldehyde at 4°C. After dehydration, bleaching and rehydration, *in situ* hybridization was performed with DIG-labeled antisense riboprobes for *Kit*, *Dct* and *MITF*. All steps except probe hybridization and final colorimetric detection were performed on a Biolane HTI (Höle & Hüttner AG, Tübingen, Germany).

Immunohistochemistry was performed on 10- $\mu$ m-thick sections from the trunk of embryos after fixation, embedding, freezing and cryotome sectioning using the following primary antibodies: anti-Islet1 mouse monoclonal (1:500 dilution, Developmental Studies Hybridoma Bank), anti-MITF rabbit antiserum (1:1000 dilution, gift of H. Arnheiter, NIH, Bethesda, MD, USA), anti-FABP7 rabbit antiserum (1:300 dilution; Millipore), anti-SOX10 guinea pig antiserum [1:1000 dilution (37)]. Secondary antibodies conjugated to Cy2, Cy3 (1:200 dilution, Dianova) or Alexa488 (1:500 dilution, Molecular Probes/Invitrogen) immunofluorescent dyes were used for detection. Nuclei were counterstained with 4',6-diamidin-2-phenylindole (DAPI).

$\beta$ -Galactosidase ( $\beta$ -gal) staining was performed on whole embryos as previously described (32).

### Cell culture and expression plasmids

MITF-M and SOX10 retroviral plasmids were described in (15,27). B22 cells were cultured as described in (38). Melb-a cells were obtained from the Wellcome Trust Functional Genomics Cell Bank (St. George's, University of London,

UK) and cultured in growth medium (RPMI 1640 with 10% fetal bovine serum, 40 pM fibroblast growth factor and 10 ng/ml stem cell factor) at 37°C under 5% CO<sub>2</sub>. Differentiation was induced when cultures were 70% confluent by replacing growth medium with differentiation medium (DMEM with 10% fetal bovine serum, 2 nM alpha melanocyte stimulating hormone (NDP-alpha MSH) and 200 nM phorbol-myristate-acetate (39). C2C12 and 3T3L1 cells were from the American Type Culture Collection (ATCC) and cultured in Dulbecco's modified Eagle's medium (DMEM) supplemented with 10% fetal calf serum.

### RNA isolation and quantitative PCR (qPCR)

Total RNA was isolated using Trizol (Life Technologies, Carlsbad, CA, USA) and cDNA was prepared using the Quantitect Reverse Transcription kit (Qiagen, Valencia, CA, USA). Quantitative PCR (qPCR) was performed in SYBR Green master mix (Qiagen) and analyzed as described (28). Primers used for mouse *Dct*: 5'-GGACCGCCCCGACTGTAATC-3' and 5'-GGGCAACGCAAAGGACTCAT-3', mouse *Tyrp1*: 5'-GCCCCAACTCTGTCTTTTCTCAAT-3' and 5'-GATCGGCGTTATACCTCCTTAGC-3', mouse *Tyrosinase (Tyr)*: 5'-CGCCCCAAATTGTACAGAGAAGC-3' and 5'-CTGCCAGGAGAAGAAGGATTG-3', mouse *Trpm1*: 5'-CCTACGACACCAAGCCAGAT-3', and 5'-GACGACACCAGTGCTCACAC-3', and mouse *Rab27a*: 5'-CGACCTGACAAATGAGCAAA-3' and 5'-GGCAGCACTGGTTTCAAAT-3'. Mouse *Mpz*, *Mbp*, and *Rpl7* primers were described in (15).

### Cell extracts and immunoblot analysis

Total cell extracts were prepared and Western blots were performed as described (28). Antiserum to BRG1 was previously described (38). The BRM and MITF antibodies were from Abcam (Cambridge, MA, USA), the SOX10 antibody was from Santa Cruz Biotechnology (Santa Cruz, CA, USA), the FLAG antibody was from Sigma (St. Louis, MO, USA), BAF60A and BAF60B antibodies were from Bethyl Laboratories (Montgomery, TX, USA) and the Tubulin antibody was from Cell Signaling Technology (Boston, MA, USA).

### Melanin assays

Cells were analyzed for melanin content as described in (40). Briefly, cells were trypsinized and counted using the Scepter 2.0 handheld automated cell counter (Millipore) Cells were lysed in 0.1 M NaOH and vortexed for 20 min. Melanin content was calculated based on the absorbance at 475 nm as compared to the standard curve obtained using synthetic melanin (Sigma, St. Louis, MO, USA) and normalized to cell number.

### siRNA knockdown

A non-targeting siRNA and siRNA targeting MITF as reported in (41–44), siRNA targeting rodent SOX10 as reported in (15,45), siBRG1/BRM as reported in (28,46) and

a SMART pool of siRNAs targeting BRG1 (siBRG1-D) were obtained from Dharmacon Inc. (Lafayette, CO, USA). Two additional siRNAs that target mouse BRG1 (siBRG1-II3.1: 5'-GUCAGACAGUAAUAAAUAAGCAA-3' and siBRG1-II3.3: 5'-GAUGAUGAGACCGUCAACCA GAUGA-3') and siRNAs that target mouse BRM (siBRM-II3.2: 5'-AUCAUUGAUACUGUGAUAAACUACA-3' and siBRM-II3.3: 5'-GAUGUGGGUGGAUAGUAU AUUUCTA-3') were purchased from Integrated DNA Technologies (Coralville, IA, USA). siRNAs were transfected with Dharmafect 1 according to manufacturer's instructions. Undifferentiated Melb-a cells were transfected in growth medium for 48 h and harvested or the medium was then replaced and the cells were cultured in differentiation medium for an additional 48 h.

### Formaldehyde-assisted Isolation of regulatory elements (FAIRE)

FAIRE was performed as essentially as described in (47). Cells were crosslinked in 1% formaldehyde for 6 min at room temperature and quenched with 125 mM glycine. Cells were then lysed using the buffers listed in the alternative lysis method as described in (48) and sonicated as described in (28). Sonicated chromatin was subjected to two rounds of phenol/chloroform extractions, back extracted once with TE and then once with chloroform. The aqueous phase was ethanol precipitated and digested with 0.2 mg/ml Proteinase K for 1 h at 55°C. Cross-links were then reversed by heating overnight at 65°C. DNA was then purified by an additional phenol chloroform extraction and ethanol precipitation. Control Inputs were 10% of each sample that was heated at 65°C overnight to reverse crosslinking prior to purification. The primers used were: mouse *Dct* distal region: 5'-ACGGTTCCACGCAAATTAAT-3' and 5'-TACTTCTCCCCATGACTGC-3', mouse *Dct* proximal region: 5'-GGCGAGCCAGAGAGAATAAA-3' A and 5'-TTCTCGCCAGTCTTCCTTGT, mouse *Tyrp1* distal region: 5'-TGACAGTGAGGGCACATTTTC-3' and 5'-ACCCATGTTCCAGACTGAA-3', mouse *Tyrp1* proximal region: 5'-GCAAAATCTCTTCAGCGTCTC-3' and 5'-AGCCAGATTCTCACACTGG-3', mouse *tyrosinase (Tyr)* distal region 5'-TGCCAGCTGACTTTGTCAAG-3' and 5'-AATATTGTGGTTTGCCAGGA-3', mouse *Tyr* proximal: 5'-AGTCATGTGCTTTGCAGAAGAT-3' and 5'-CAGCCAAGAACATTTCTCCTT-3' mouse *Scn2a1*: 5'-AAGCAGCTGCCTTTGGGAAG-3' and CACAGCACTGAGCATCAAG-3' and mouse *MyoD* CER as reported in (49).

### Chromatin immunoprecipitation (ChIP)

ChIP was performed as described (28) using the same antibodies as in Westerns as well as antibodies to histone H3, H3K4me3 and H3K27ac that were obtained from Abcam. Primers were the same as used in FAIRE.

### Statistical analysis

Statistical significance was calculated by the Student's *t* test. One way ANOVA followed by Tukey's post-hoc test was used for comparing multiple groups.

## RESULTS

### ENU alleles of *Smarca4*

We used a previously established *N*-ethyl-*N*-nitrosourea (ENU) mutagenesis screen to identify novel modifiers of *SOX10* neurocristopathies (Mos) (32). Briefly, BALB/cJ male mice were given weekly ENU injections for 3 weeks, and after regaining fertility, mated with C57BL/6J females to generate first generation (G<sub>1</sub>) offspring. G<sub>1</sub> males were mated with *Sox10*<sup>LacZ/+</sup> females and second generation (G<sub>2</sub>) offspring were then scored for hypopigmentation. One of the founder mutants, *Mos6*, had more severe white spotting than is typically observed in the *Sox10*<sup>LacZ/+</sup> haploinsufficient mice (Figure 1A). Further breeding of this founder and quantitation of ventral spotting in the pedigree showed that *Mos6* synergistically increased the severity of white spotting observed in *SOX10* haploinsufficient mice (Figure 1B). To map the *Mos6* locus, seven affected *Mos6*<sup>+/+</sup>; *SOX10*<sup>LacZ/+</sup> double heterozygotes were genotyped in a low density genome scan (61 simple sequence length polymorphism markers), and in parallel with this linkage mapping, one *Mos6*<sup>+/+</sup>; *SOX10*<sup>LacZ/+</sup> double heterozygote sample was used for exome sequencing. Candidate sequence variants within regions of potential linkage were further refined by subsequent breeding that confirmed linkage of *Mos6* to two sequence variants within *Smarca4*, the gene that encodes BRG1.

The two *Smarca4* ENU mutations include a splice site variant at the consensus 5' donor splice site of exon 11 (mm9 Chr9:21447196;G>T) as well as a downstream variant in exon 22 (mm9 Chr9:21474974;G>A). Subsequent genotyping of both *Smarca4* ENU mutations confirmed strong linkage with the *Mos6* phenotype throughout the colony (0/42 recombinants over three generations;  $\chi^2 = 42$ ;  $P < 0.0001$ ). Because of the proximity of the two ENU mutations within *Smarca4*, they could not be segregated in the colony and thus we could not determine the relative contribution of the two mutations individually to the phenotype. However, the splice site variant at the junction of exon 11 and intron 11 (c.1812+1G>T, NM\_001174078.1) is predicted to introduce a frameshift resulting in protein truncation upstream of the variant in exon 22, thus rendering the exon 22 variant incapable of contributing to the *in vivo* phenotype. To confirm the consequence of the splice site variant, RT-PCR products from *Mos6* heterozygotes were sequenced. There was no evidence of exon skipping or intron retention resulting from the splice site variant, however, a mutant transcript was detected that results from activation of a cryptic splice site 5 bp upstream of the Exon 11 splice site disrupted by the mutation (Figure 1C). The ratio of chromatogram peaks detected by sequencing of the RT-PCR product suggested that the mutant transcript was present at low levels (~15% of the total transcript (Figure 1C)). To further characterize the stability of this *Mos6* mutant transcript, the relative ratio of wild type and mutant transcript was measured in an outcross to FVB/N, where a strain-specific SNP (rs48515263) within exon 15 of *Smarca4* could be used to assess relative expression of the two alleles. In cDNA from a wild-type F1 hybrid embryo, the two SNP alleles (C57BL/6J and FVB/N) were detected in equal proportion. In contrast, cDNA from

a *Mos6* heterozygous F1 hybrid embryo confirmed that the C57BL/6J SNP allele carrying the linked *Mos6* mutations was barely detectable relative to the FVB/N wild-type allele, thus indicating that the mutant transcript was unstable (Figure 1D). Consistent with this, Western blotting failed to detect any evidence of the truncated protein (605 aa for *Smarca4* mutant versus 1617 aa for wild-type) that might result from any residual *Mos6* mutant transcript (Figure 1E). In summary, the low levels of mutant transcript along with the negative Western data indicate that the splice site mutation is likely responsible for the phenotype observed in *Mos6* mice and that the *Mos6* allele is functionally null. We subsequently use the allele name *Smarca4*<sup>Mos6</sup> to refer to the allele that contains both point mutations.

Because of the visible white spotting in *Smarca4*<sup>Mos6/+</sup>; *Sox10*<sup>LacZ/+</sup> double heterozygote adult mice, we sought to further characterize the effect of *Smarca4* mutation on melanocyte development. A reduction in melanoblasts was first evident at E13.5 when the number of cranial melanoblasts marked by whole mount  $\beta$ -gal staining was significantly reduced in *Smarca4*<sup>Mos6/+</sup>; *Sox10*<sup>LacZ/+</sup> double heterozygotes compared to *Sox10*<sup>LacZ/+</sup> heterozygotes (Supplementary Figure S1). The reduction in melanoblast number was *Sox10*-dependent, as a similar reduction was not observed in *Smarca4*<sup>Mos6/+</sup> heterozygote embryos where melanoblasts were marked with a *Dct-LacZ* transgene (data not shown). Further characterization of melanoblast development was limited as we were not able to recover *Smarca4*<sup>Mos6/Mos6</sup> homozygous embryos at E9.5 or later time points, consistent with published observations of early embryonic lethality resulting from a *Smarca4* null allele (31),

### Conditional deletion of *Smarca4* in melanoblasts

To further characterize the impact of *Smarca4*-deficiency on melanocyte development and confirm *Smarca4*<sup>Mos6</sup> as the causative mutation for the *Mos6* phenotype, we characterized a second allele of *Smarca4*. Melanocyte development was examined when *Smarca4* was specifically deleted in *SOX10*-expressing cells using a *SOX10*-Cre construct (33,34). This conditional deletion of *Smarca4* and subsequent loss of BRG1 expression resulted in a striking reduction in the numbers of cranial and ventral trunk melanoblasts at E12.5 as visualized by *Mitf*, *Dct* and *Kit in situ* hybridization (Figure 2A and B). Quantification of cells in the eye region that were positive for *Mitf*, *Dct* and *Kit* revealed a drastic reduction of melanocytes (Figure 2B, region 1). *Mitf*-positive cells were reduced to  $1.3 \pm 0.7\%$ , *Dct*-positive cells to  $1.6 \pm 0.4\%$  and *Kit*-positive cells to  $13.0 \pm 8.8\%$  (Figure 2C). Immunohistochemistry of trunk sections indicated a less pronounced, but qualitatively similar reduction of *Mitf*-positive cells to  $43.6 \pm 10.6\%$  (Supplementary Figure S2). This correlates with a *Sox10*-Cre mediated deletion rate of  $57 \pm 5\%$  ( $n = 3$ ) that we determined for a *Rosa26*-stopflox-YFP reporter in trunk melanocytes (data not shown). We also investigated the consequences of the *Smarca4* deletion on other neural crest lineages as well as the possibility of a fate switch in melanoblasts. However, FABP7-expressing Schwann cell precursors along peripheral nerves (Supplementary Figure S3A, left) and ISLET1-

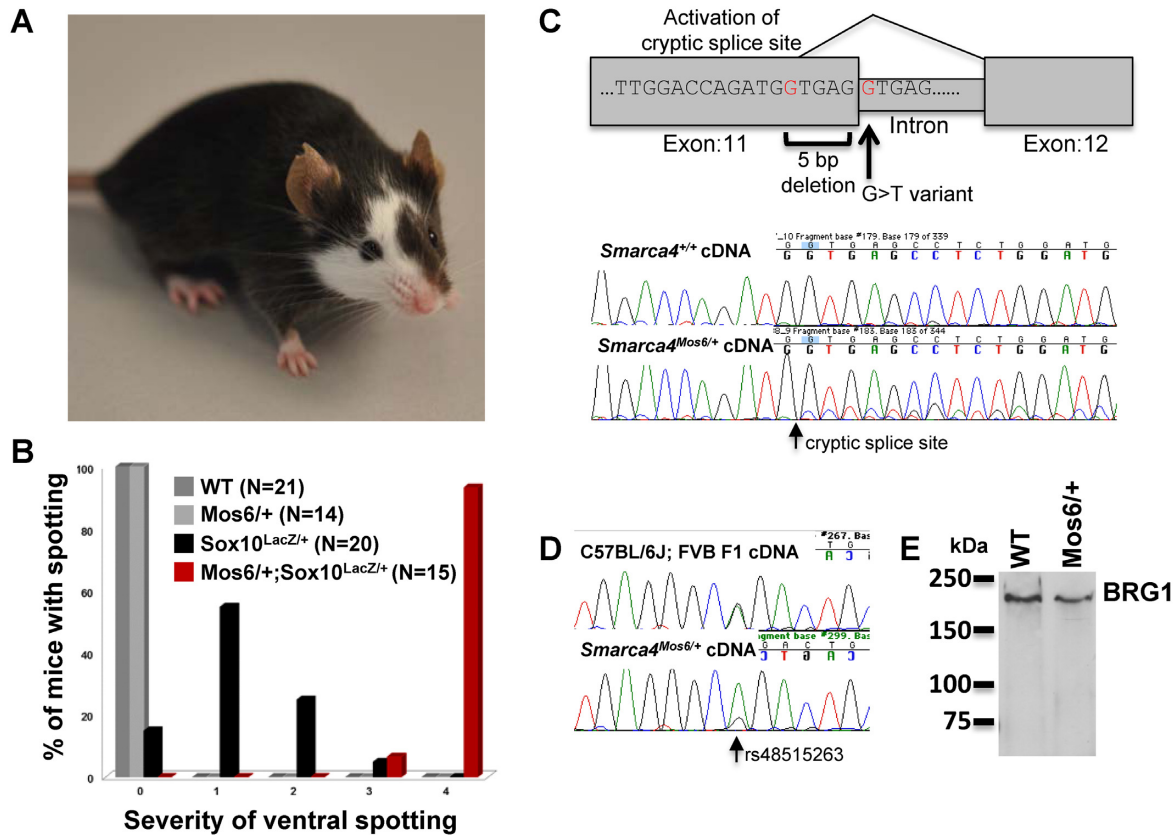


**Figure 1.** Identification of the *Smarca4*<sup>Mos6</sup> allele. (A) *SOX10*<sup>LacZ/+</sup>; *Mos6*<sup>+/+</sup> double heterozygous mice exhibited a head spot and extensive belly spotting, demonstrating that the presence of the *Mos6* allele increased the spotting phenotype of *SOX10*<sup>LacZ/+</sup>. (B) Hypopigmentation in the trunk of adult mice was quantitated using a standardized scale of 0–4, in which 0 indicates no spotting, and 1–4 indicates progressively greater hypopigmentation (32). *Mos6* synergistically increased the ventral white spotting observed in *SOX10* haploinsufficient mice. (C) The *Smarca4* mutation splice site variant (mm9 Chr9:21447196;G>T) that alters a consensus 5' donor splice site at the junction of exon 11 and intron 11 (c.1812+1G>T, NM.001174078.1). Low levels of a mutant transcript were detected (15% of total transcript), suggesting the mutant causes activation of a cryptic splice site within exon 11, as illustrated. (D) In cDNA from an outcross C57BL/6J and FVB/N F1 hybrid embryo, the two strain-specific alleles at rs48515263, a SNP located within exon 15 of *Smarca4*, were present in equal proportion. In cDNA from an embryo carrying the *Mos6* ENU-induced C57BL/6J mutation, the C57BL/6J SNP allele detected in the mutant transcript was reduced relative to the FVB/N wild-type allele, consistent with instability of the *Mos6* mutant allele. (E) Western blots detected only wild-type BRG1 expressed in *Mos6*<sup>+/+</sup> heterozygous embryos. Similar results were observed using four embryos of each genotype run in triplicate Western blots with no detection of a truncated protein even with overloading or overexposure.

positive sensory neurons in dorsal root ganglia (Supplementary Figure S2B) are still present in the *Smarca4*-deleted mice despite near complete deletion of the *Rosa26*-stopfloxed-YFP reporter. We also have no evidence that the remaining melanocytes convert to FABP-expressing glia (Supplementary Figure S3A, right) or islet1-expressing neurons (data not shown). This conditional *Smarca4* mutant verifies the causative mutation in *Mos6* mice and confirms an essential role for the *Smarca4*-encoded protein, BRG1, in establishing the SOX10-expressing melanoblast lineage.

#### The requirement for BRG1 in the activation of melanocyte-specific genes by SOX10

To elucidate the transcriptional mechanisms by which BRG1 cooperates with SOX10 to establish the melanocyte lineage, we turned to a previously described fibroblast cell line that can be induced to express a dominant negative version of BRG1 under the control of the tetVP16 activator, hereafter referred to as dnBRG1 (38). dnBRG1 lacks chromatin remodeling activity due to a mutation in

the ATPase domain and acts as a dominant negative because it suppresses gene activation events that normally require SWI/SNF function. By ectopically expressing either SOX10 or MITF in B22 cells, we previously found that SOX10 interacts with BRG1 to promote myelin gene expression while MITF interacts with BRG1 to promote melanocyte-specific gene expression (15,27). To determine the requirement for BRG1 in SOX10-mediated melanocyte-specific gene expression, we ectopically expressed MITF, SOX10, or a combination of MITF and SOX10 in B22 cells and cultured them in the presence or absence of tetracycline. Western blotting confirmed that MITF, SOX10, or both MITF and SOX10 were expressed regardless of the presence or absence of tetracycline, while expression of dnBRG1 was detected only in cells that had been cultured in the absence of tetracycline (Figure 3A).

Consistent with our previous semi-quantitative data (27), we found that ectopic expression of MITF in B22 cells that were cultured in the presence of tetracycline activated expression of tyrosinase family members *Dct* (110-fold), *Tyrp1*

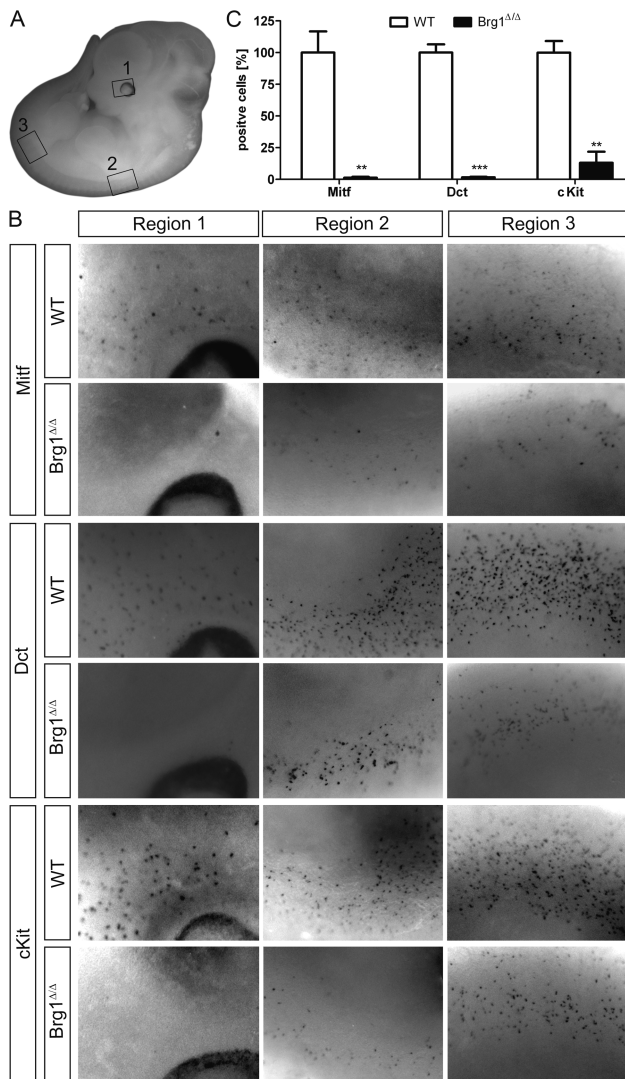


**Figure 2.** Conditional deletion of *Smarca4* resulted in a striking reduction in the numbers of cranial and ventral trunk melanoblasts at E12.5. (A) The melanoblast-containing regions labeled 1 (cranial melanoblasts near optic cup), 2 (anterior trunk at forelimb) and 3 (posterior trunk at hindlimb) are shown at greater magnification in B, as indicated. (B) Comparison of melanoblast number, as measured by whole mount *in situ* hybridization for *MITF* (top), *Det* (center) and *Kit* (bottom) shows fewer melanoblasts in embryos where *Smarca4* was conditionally deleted in melanoblasts using a SOX10-Cre construct (*BRG1<sup>Δ/Δ</sup>*) as compared to normal littermates (WT). (C) Quantification of cells in the eye region from the ISH whole mounts that were positive for the indicated melanocyte markers (\*\*\*)  $P < 0.001$ , \*\*  $P < 0.01$ , Student's *t* test).

(600-fold) and *Tyr* (20-fold) and removal of tetracycline and expression of dominant negative BRG1 dramatically inhibited expression of these three genes (Figure 3B). SOX10 is known to induce *Mitf* expression when partnered with PAX3 (50). We found that in the absence of Pax3, ectopic expression of SOX10 increased *Mitf* expression <2-fold compared to a control empty vector (data not shown). Interestingly, SOX10 induced expression of MITF target genes to a greater extent (Figure 3B). *Dct* was activated by SOX10 (57 000-fold) which was greater than *Dct* activation by MITF. However, SOX10 was less effective than MITF in activating

*Tyrp1* (100 fold) and *Tyr* (5-fold). Co-expression of MITF and SOX10 resulted in a synergistic increase in *Dct* expression (300 000-fold), *Tyrp1* (2000-fold) and *Tyr* (350-fold). Activation of these three genes by MITF, SOX10 or MITF in combination with SOX10 was dramatically inhibited by expression of dnBRG1. These data suggest that BRG1 functionally interacts with SOX10 and that its catalytic activity is required for expression of the MITF- and SOX10-regulated genes that encode enzymes involved in melanin synthesis.

We also investigated whether SOX10 could activate the expression of two other MITF target genes that are important for melanocyte function. The transient receptor potential cation channel member 1 (*Trpm1*), associated with terminal melanocyte differentiation, and the small GTPase, *Rab27a*, which regulates melanosome transport are known MITF target genes (51–53). We found that MITF induced *Trpm1* (200-fold) and *Rab27a* (80-fold) in a BRG1-dependent manner (Figure 3C). However, the expression of these genes did not change significantly in SOX10 expressing cells relative to control. The combination of MITF and SOX10 increased the mRNA levels of *Trpm1* and *Rab27a* to a small extent (1.6- and 1.25-fold respectively) compared to the levels induced by MITF alone. Thus, expression of *Trpm1* and *Rab27a* is highly dependent on MITF and BRG1 but less so on SOX10 in these cells.

Our previous work had indicated that ectopic expression of SOX10 in B22 cells can induce expression of Schwann cell genes that encode myelin protein zero (*Mpz*) and myelin basic protein (*Mbp*) (15). These genes were recently found to be regulated by MITF in melanoma cells (54,55). Therefore, we queried whether SOX10 synergizes with MITF to increase expression of *Mpz* and *Mbp* in a BRG1-dependent manner. We found that MITF alone did not significantly induce either *Mpz* or *Mbp* (Figure 3D). As we determined previously, SOX10 activated both *Mpz* and *Mbp* when cells were cultured in the presence of tetracycline but not when expression of dnBRG1 was induced by the removal of tetracycline. Interestingly, co-expression of MITF with SOX10 prevented SOX10 from inducing these myelin genes. Thus, in this cellular context, SOX10 cooperates with MITF to activate a subset of melanocyte-specific genes in a BRG1-dependent manner but works antagonistically with MITF to regulate genes important for myelination.

### Temporal analysis of melanin synthesis and gene expression in differentiating melanoblasts

*In vitro* models of muscle and adipocyte differentiation, such as C2C12 myoblasts and 3T3L1 pre-adipocytes, have provided a wealth of knowledge regarding the mechanisms by which previously silent genes embedded in repressive chromatin structure are activated in a lineage-specific manner (25,56–58). However, *in vitro* models of melanocyte differentiation have been rarely used for such purposes. Therefore, we characterized mouse Melb-a cells, which are immortalized mouse melanoblasts derived from black nonagouti mice (39,59), to elucidate the mechanisms by which BRG1 co-activates SOX10 target genes in melanocytes. These cells can be maintained in an undifferentiated proliferative state when cultured in growth medium

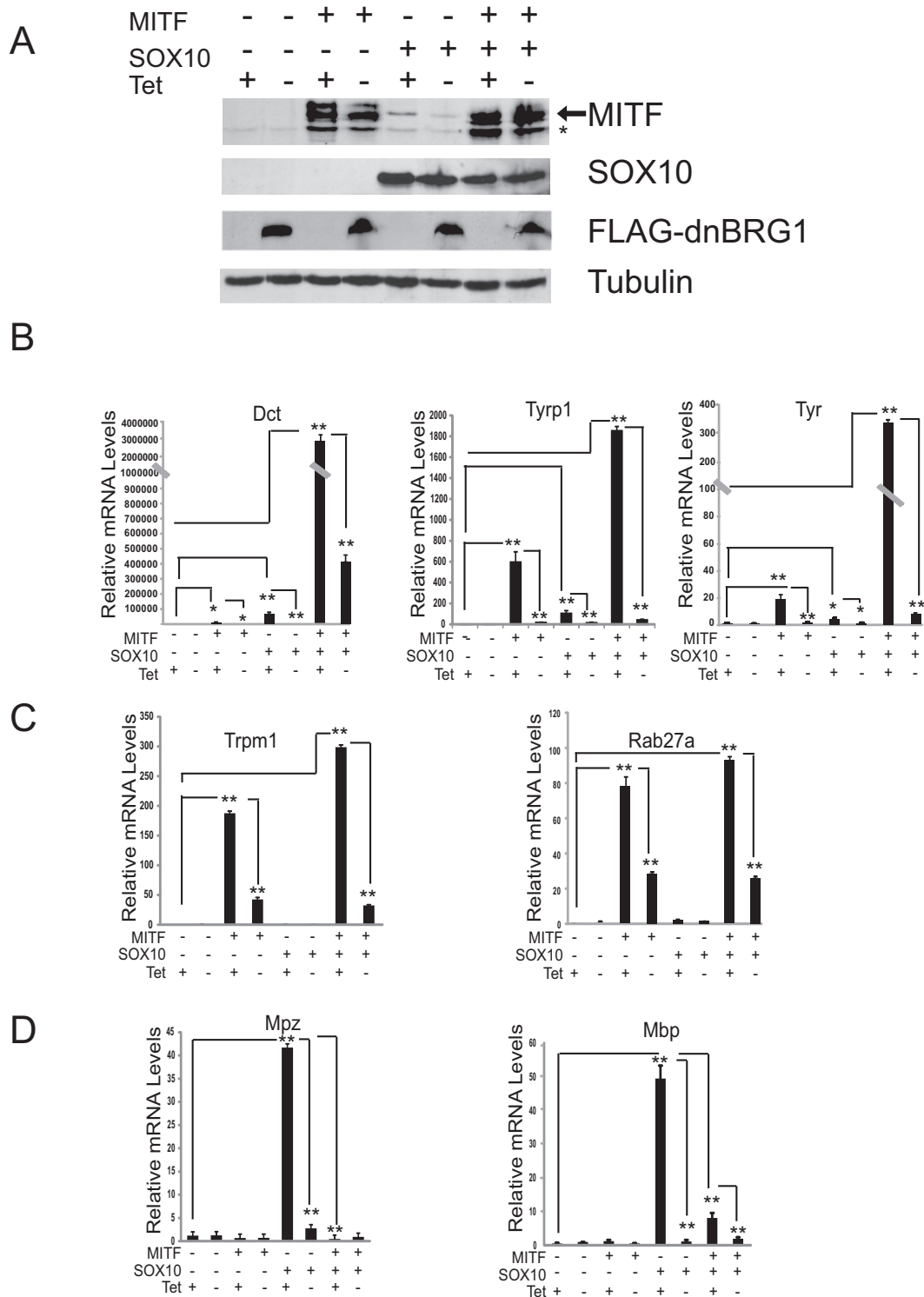


**Figure 3.** Dominant negative BRG1 inhibits activation of melanocyte-specific genes by MITF and SOX10. (A) B22 cells were infected with a pBABE control vector, pBABE-MITF, pBABE-SOX10 or pBABE-MITF with pBABE-SOX10 in the presence (dominant negative BRG1 off) or absence of tetracycline (dominant negative BRG1 on) and then cultured in low serum medium to promote differentiation. Western Blot analysis showing expression of MITF and SOX10 in cells that were cultured in the presence and absence of tetracycline, and the expression of FLAG-tagged dominant BRG1 when cells were cultured in the absence of tetracycline. Protein expression was detected from cell extracts and tubulin was used as a loading control. (B–D) Quantitative RT-PCR (qRT-PCR) of MITF and/or SOX10 target genes from cells transfected with pBABE, pBABE-MITF, pBABE-SOX10 or pBABE-MITF together with pBABE-SOX10 in the presence or absence of tetracycline demonstrated that dominant negative BRG1 blocked the (B) synergistic activation of *Dct*, *Tyrp1* and *Tyr* gene expression by SOX10 and MITF, (C) activation of *Trpm1* and *Rab27a* by MITF and (D) activation of *Mpz* and *Mbp* by SOX10. Expression of each gene was normalized to expression of *Rpl7*. The data are the average of at least two independent experiments performed in triplicate. Standard error bars and statistical significance are shown (\*\* $P < 0.01$ , \* $P < 0.05$ , ANOVA).

containing stem cell factor (SCF) and fibroblast growth factor 2 (FGF2) and then differentiated into pigmented melanocytes by shifting sub-confluent cells to differentiation medium containing a stable analog of alpha-MSH (NDP- $\alpha$ -MSH). We observed a time-dependent increase in melanin accumulation when Melb-a cells were shifted from growth to differentiation medium (Figure 4A). MITF expression was strongly induced concomitantly with the observed increase in melanin synthesis while SOX10 levels and BRG1 levels remained constant (Figure 4B). Interestingly, there was a small increase in the expression of the alternative ATPase BRM after 24 h of differentiation, suggesting that BRM may have a role in melanocyte differentiation (Figure 4B).

We performed a temporal analysis of gene expression to determine if genes required for melanin synthesis are induced during the differentiation process. Our data indicate that expression of these genes increases over a 48-h time period (Figure 4C and D). This long time-course of gene induction is likely due to asynchronous differentiation of individual cells as was previously demonstrated for B16 melanoma cells (60). Induction of *Dct* and *Tyrp1* expression occurred 12 h after shifting to differentiation medium and peaked after 24 h with a 7–8-fold induction of *Dct* and 50–60-fold induction of *Tyrp1*, while *Tyr* expression was first detected at 24 h but increased substantially after 48 h with an ~120-fold induction (Figure 4C). *Rab27a* and *Trpm1* were induced with similar kinetics as *Dct* and *Tyrp1*, with a maximum induction of 8-fold and 50-fold respectively (Figure 4D). Whereas these MITF-dependent genes were consistently induced during the time course of Melb-a differentiation, the expression of *Mpz*, a gene which was activated by SOX10 but repressed by MITF in B22 cells, decreased during the time course of Melb-a differentiation while *Mbp* levels fluctuated and exhibited a slight increase of 1.5-fold after 48 h (Figure 4E).

#### Temporal analysis of gene expression and chromatin accessibility in differentiating melanoblasts

We performed a temporal analysis of chromatin accessibility in differentiating Melb-a cells to determine if the observed changes in melanocyte-specific gene expression were associated with alterations in chromatin structure. The FAIRE (Formaldehyde-Assisted Isolation of Regulatory Elements) assay enriches for accessible chromatin sites that correspond closely with DNase I hypersensitive sites, occurring at transcriptional start sites, promoters, and enhancers (61). We assayed the regions of *Dct*, *Tyrp1* and *Tyr* that contain SOX10 and MITF binding sites: SOX10 binding sites are located in distal enhancers, while M boxes which bind MITF are located in proximal promoter regions and E boxes that also bind MITF are also contained within distal enhancers (50,62–65). We detected significant FAIRE enrichment of the *Dct* distal enhancer and proximal promoter both in undifferentiated and in differentiated Melb-a cells but not in myoblasts (C2C12) nor pre-adipocytes (3T3L1). (Figure 5A). There was only a small increase in the FAIRE enrichment of the distal enhancer after 48 h of differentiation while enrichment of the *Dct* proximal promoter increased ~2-fold. The enrichment level of the *Tyrp1* distal

enhancer was also high in undifferentiated Melb-a cells but not in C2C12 or 3T3L1 cells and increased slightly during the time course of differentiation, whereas there was a significant increase in the enrichment level of the *Tyrp1* proximal promoter during the time course of differentiation (3-fold) (Figure 5B). We digested nuclei with MNase I and confirmed that FAIRE enrichment levels of the *Tyrp1* distal and proximal regions reflect changes in chromatin accessibility (data not shown). Similarly, enrichment of the *Tyr* distal enhancer was high in undifferentiated Melb-a cells compared to C2C12 and 3T3L1 cells and increased to a small extent during differentiation, while enrichment of the *Tyr* proximal promoter was only slightly higher in undifferentiated Melb-a cells than in C2C12 and 3T3L1 cells and increased greatly (7-fold) during the time course of differentiation (Figure 5C). Thus, the distal enhancers of *Dct*, *Tyrp1* and *Tyr* were observed to be in a constitutively open chromatin state prior to differentiation while the chromatin at the proximal promoters of the highly induced *Tyrp1* and *Tyr* became increasingly accessible upon differentiation. As a control for FAIRE specificity, we probed a distal regulatory region (CER) of *MyoD*, a muscle-specific gene that is expressed in proliferating C2C12 myoblasts (49). As expected, we found high FAIRE enrichment of this region in C2C12 cells compared to Melb-a and 3T3L1 cells (Figure 5D) while the level of FAIRE enrichment of the control *Scn2a1* upstream region was similarly low in all cells (Figure 5E).

We confirmed FAIRE analysis with chromatin immunoprecipitations (ChIPs) to detect histone modifications that are associated with active gene expression. Active enhancers are marked by high levels of histone H3 acetylated on lysine 27 (H3K27ac) and low levels of histone H3 trimethylated on lysine 4 (H3K4me3), while active promoters are marked by high levels of H3K4me3 and variable levels of H3K27ac (66). We found that the distal enhancers of *Dct*, *Tyrp1* and *Tyr* had low levels of H3K4me3 and high levels of H3K27ac which did not significantly increase (*Dct*, Figure 6A, left) or increased to a small extent upon differentiation (*Tyrp1*, Figure 6B, left, *Tyr*, Figure 6C, left). The proximal promoters of *Dct*, *Tyrp1* and *Tyr* displayed variable increases in both H3K27ac and H3K4me3 enrichment upon differentiation, with *Tyr* characterized by the lowest relative levels of these histone modifications in undifferentiated Melb-a cells and the highest relative increase upon differentiation (Figure 6A, B, C, right). ChIP specificity was demonstrated by low enrichment of melanocyte-specific regulatory regions and high H3K27ac enrichment of the *MyoD* CER in C2C12 cells (Figure 6D) and low enrichment of the *Scn2a1* locus in all cells (Figure 6E). These experiments confirm FAIRE analysis which suggests that the distal regulatory regions of melanocyte-specific genes are primed by open chromatin structure in undifferentiated melanoblasts, while proximal promoters become increasingly accessible upon differentiation.

#### Depletion of SOX10 and BRG1 inhibits melanocyte differentiation and melanocyte-specific gene expression

To investigate the requirement for SOX10 and BRG1 in Melb-a differentiation, we depleted expression of these proteins by transiently transfecting short interfering RNAs



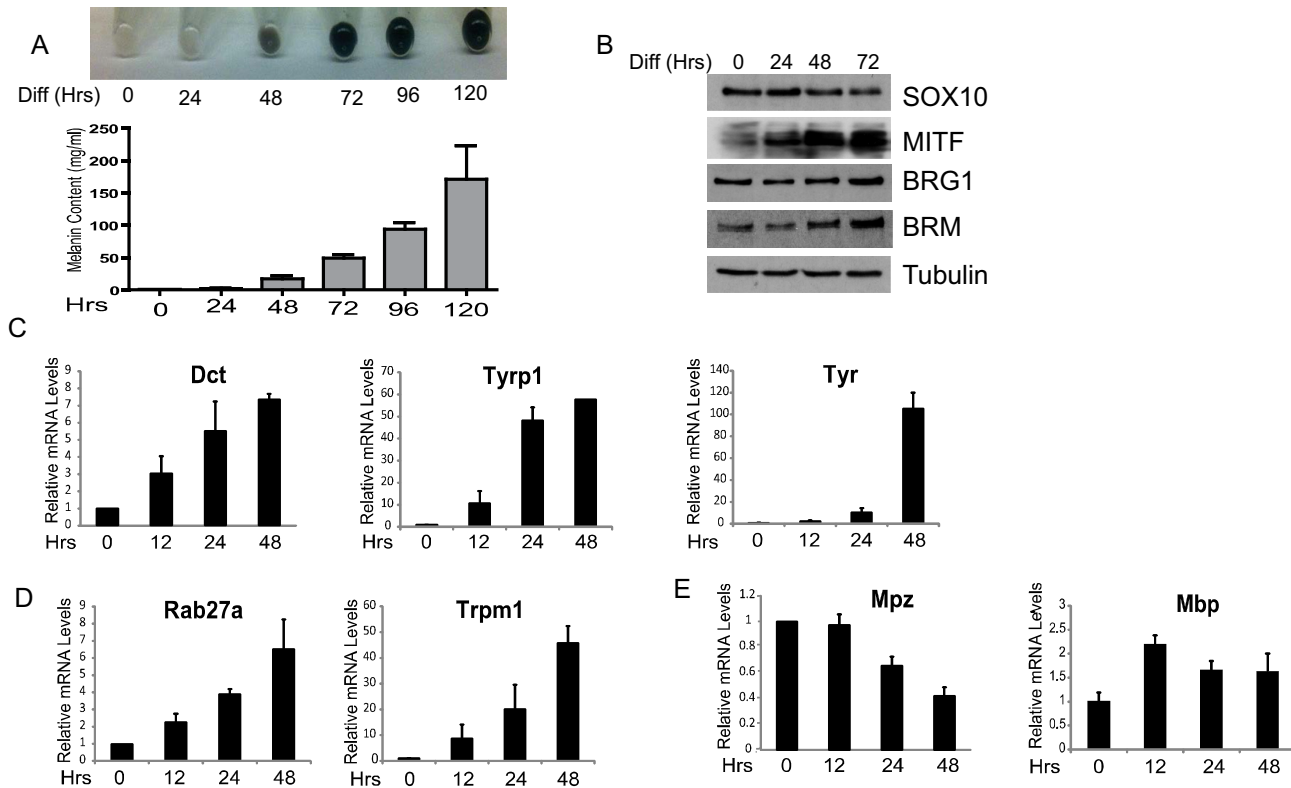


**Figure 4.** Melanin synthesis and changes in gene expression during a time course of melanoblast differentiation (A) Melb-a cells were cultured in growth medium containing SCF and FGF until 70% confluent (time 0), then growth medium was replaced with differentiation medium containing NDP- $\alpha$ -MSH and the cells were cultured for the indicated periods of time. Cells were harvested at each time point and photographed. Cells were counted and an equal number were subjected to the melanin assay. The data are the average of at least two independent experiments performed in triplicate. Standard error bars and statistical significance compared to siC are shown (\*\* $P < 0.01$ , \* $P < 0.05$ , Student's  $t$  test). (B) Protein extracts were prepared from differentiating Melb-a cells and subjected to Western blotting with the indicated antibodies. Tubulin was used as a loading control. (C–E) RNA was isolated at the indicated time points, reverse transcribed and the specific transcript of interest quantified by qRT-PCR. The CT value for each gene was normalized to *Rpl7*. The data are the average of at least two independent experiments performed in triplicate. (C) Melanogenic enzyme gene expression increased as the cells differentiated. (D) Expression of genes associated with melanocyte differentiation increased as the cells differentiated. (E) Expression of myelin genes either decreased (*Mpz*) or exhibited a transient modest increase (*Mbp*). Standard error bars and statistical significance compared to siC are shown (\*\* $P < 0.01$ , \* $P < 0.05$ , Student's  $t$  test).

(siRNA). Because SOX10 regulates MITF expression, we also knocked down MITF to compare the effects of concurrent depletion of SOX10 and MITF with depletion of MITF alone. Furthermore, because our previous data in melanoma cells suggested that the alternative ATPase, BRM, can partially compensate for BRG1 loss (28), we utilized a siRNA sequence that targets only BRG1 and an siRNA sequence that targets both BRG1 and BRM. These siRNAs or a non-targeting siRNA (siC) were transfected into undifferentiated Melb-a cells and then cells were shifted to differentiation medium 48 h later. The extent of knockdown was evaluated by Western blotting (Figure 7A and B). Knockdown of SOX10, BRG1 or BRG1/BRM inhibited MITF expression in Melb-a cells and knockdown of BRG1 or BRG1/BRM also caused a small decrease in SOX10 expression (Figure 7A). These results are consistent with other reports that SOX10 transcriptionally activates MITF expression (67) and that BRG1 can also contribute to the regulation of MITF and SOX10 in melanoma (68) and Schwann cells (69) respectively. However, it is important to note that the effect of BRG1 or BRG1/BRM depletion on the expres-

sion of either MITF or SOX10 was small compared to the effects seen by depletion with siMITF or siSOX10.

We then assayed the effects of the knockdowns on melanin content (Figure 7B). Transfection with siSOX10, which not only depleted SOX10 but also severely inhibited MITF expression, had a slightly greater effect on observable pigmentation than transfection of siMITF which depleted MITF but did not affect SOX10 expression. Depletion of both BRG1 and BRM had a greater effect on observable pigmentation compared to depletion of BRG1 alone, suggesting that BRM may contribute to activation of genes required for melanin synthesis.

To more precisely determine the relative contributions of BRG1 and BRM in promoting pigmentation and melanin synthesis, we utilized additional siRNAs that uniquely target each of the ATPases. Two siRNAs against BRG1 (siBRG1-II3.1 and siBRG1-II3.3) and two siRNAs directed against BRM (siBRM-II3.2) and siBRM-II3.3 depleted the respective proteins with varying efficiencies (Figure 7C). Depletion of BRG1 by either siBRG1-II3.1 or siBRG1-II3.3 reduced MITF, TYRP1 and TYR at the protein level, but had only a slight effect on SOX10 expression, while de-

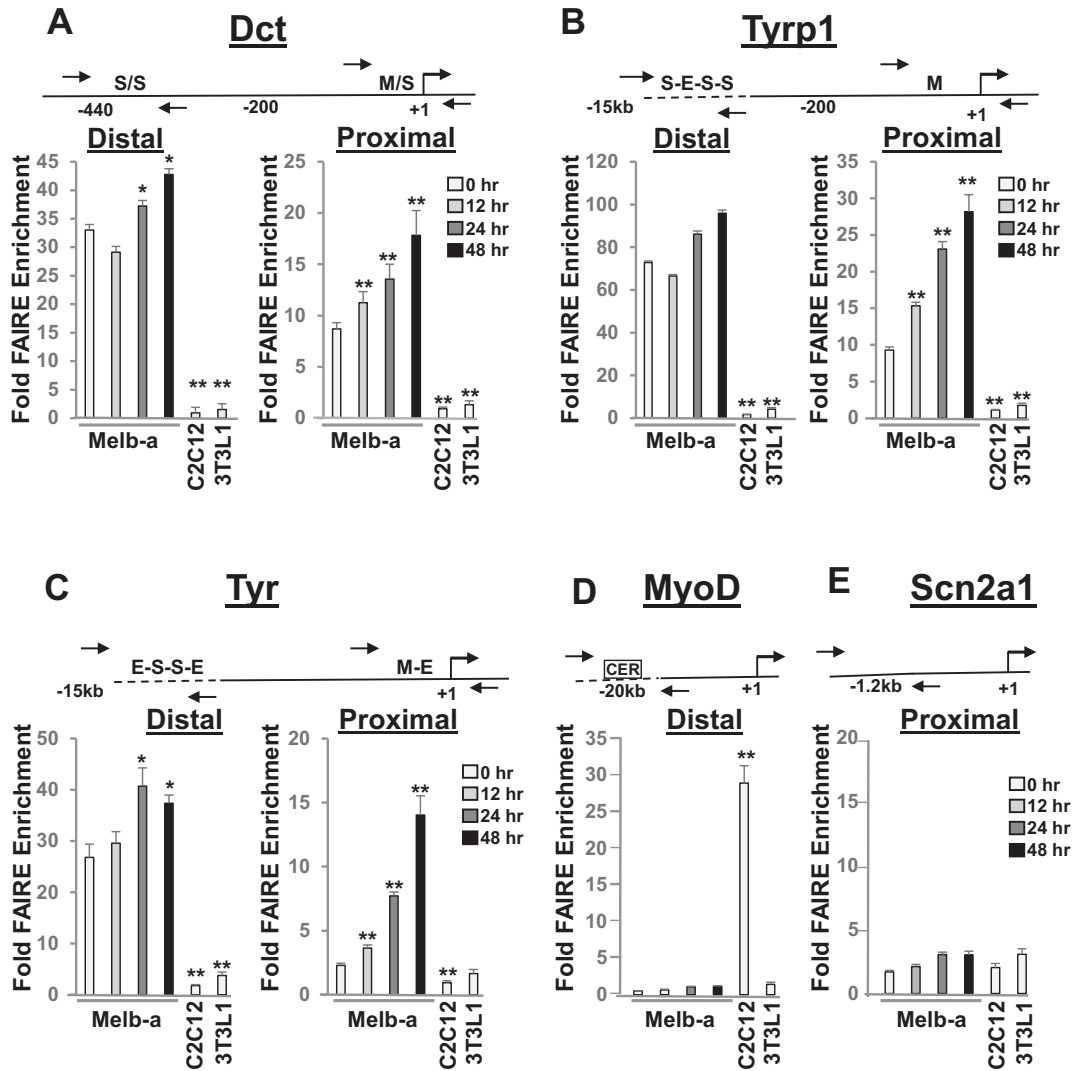


**Figure 5.** Time course of chromatin accessibility at distal and proximal control regions of melanogenic enzyme genes during Melb-a differentiation. (A–C) Melb-a cells were cultured in growth medium containing SCF and FGF2 until 70% confluent (time 0). Growth medium was replaced with differentiation medium containing NDP- $\alpha$ -MSH and the cells were cultured for the indicated periods of time. C2C12 and 3T3L1 cells were cultured in growth media and harvested at 70% confluency. Cells were cross-linked and subjected to FAIRE analysis. Enrichment was quantified by qPCR by normalizing to an input (UnFAIRE) control for each primer set. A schematic of the distal enhancer and proximal promoter elements for each locus is shown above each graph. (A) *Dct*, (B) *Tyrp1*, (C) *Tyr*. (D) *MyoD*, (E) *Scn2a1* (M: Mbox, S: SOX10 binding site, E: E box). The data are the average of at least two independent experiments performed in triplicate. Standard error bars and statistically significant differences compared to undifferentiated (0hr) Melb-a cells are shown (\*\* $P < 0.01$ , \* $P < 0.05$ , Student's *t* test).

pletion of BRM by either siRNA had minimal effects on MITF and SOX10. Only the more efficient siBRM-I13.3 substantially reduced TYRP1 and TYR expression at the protein level. Depletion of BRG1 by either siRNA reduced observable pigmentation and melanin content while only the more efficient siRNA targeting BRM had an inhibitory effect on observable pigmentation and on melanin content (Figure 7D).

We next investigated the effects of the knockdowns on expression of SOX10 and MITF target genes. As expected, knockdown of either SOX10 or MITF inhibited expression of genes that regulate melanin synthesis and melanocyte function (Figure 7E and F). Knockdown of BRG1 by either siBRG1-D (60% knockdown by qRT-PCR, data not shown) or siBRG1-I13.1 (80% knockdown by qRT-PCR,

data not shown) significantly reduced expression of these genes such that the more efficient knockdown of BRG1 resulted in a greater effect on melanocyte-specific gene expression (Figure 7E and F). Knockdown of BRM alone by either siBRM-I13.2 (65% knockdown by qRT-PCR, data not shown) or siBRM-I13.3 (80% knockdown by qRT-PCR) resulted in small but significant effects on most melanocyte-specific genes. Therefore, both BRG1 and BRM likely contribute to the regulation of these melanocyte-specific genes, with BRG1 depletion having a more severe effect on expression of DCT, TYRP1 and TYR at both the protein and gene levels as well as on observable pigmentation.

Consistent with the inhibitory effect of MITF expression on *Mpz* and *Mbp* expression in NIH 3T3 cells (Figure 3D), we found that knockdown of MITF in Melb-a cells led to

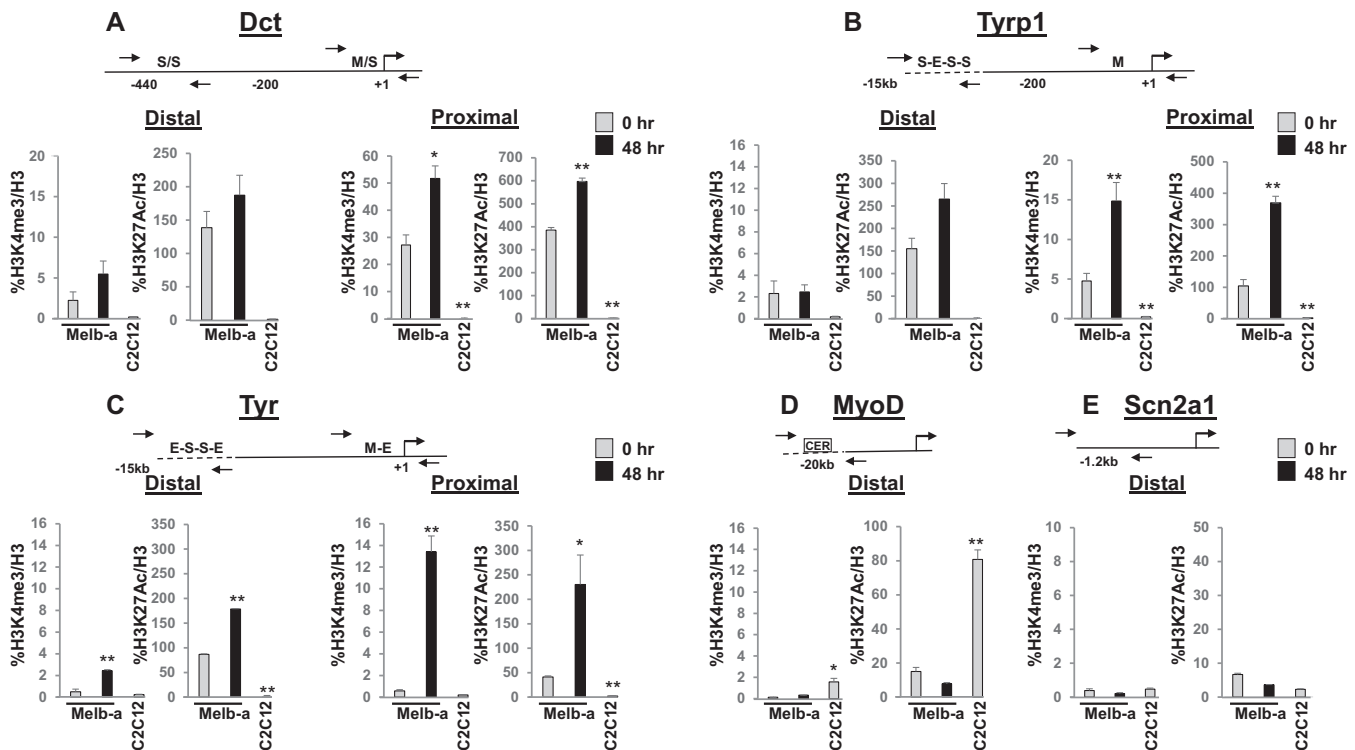


**Figure 6.** Changes in histone modifications at distal and proximal control regions of melanogenic enzyme genes during Melb-a differentiation. Chromatin immunoprecipitations (ChIPs) were performed with antibodies to histone H3, histone H3 acetylated on lysine 27 (H3K27ac), histone H3 trimethylated at lysine 4 (H3K4me3), or a control IgG antibody. Enrichment was quantified by qPCR by normalizing to H3 for each primer set. ChIP with IgG resulted in < 1% of the enrichment obtained with histone antibodies (data not shown). (A) *Dct*, (B) *Tyrp1*, (C) *Tyr*, (D) *MyoD* CER, (E) Upstream region of *Scn2a1*. The data are the average of at least two independent experiments performed in triplicate. Standard error bars and statistical significance compared to undifferentiated (0hr) Melb-a cells are shown (\*\* $P < 0.01$ , \* $P < 0.05$ , Student's *t* test).

an increase in the expression of these genes, while knock-down of SOX10, BRG1 and BRM decreased their expression (Figure 7G). Ectopic expression of MITF in SOX10-depleted cells partially restored *Dct*, *Tyrp1*, *Tyr* and *Trpm1* expression and fully restored *Rab27a* levels to those in cells expressing control siRNA (siC), but did not have a significant effect on the expression of *Mpz* and *Mbp* (Figure 7H). These data show that MITF cannot fully compensate for SOX10 loss in the regulation of a subset of melanocyte-specific genes that require BRG1, including *Dct*, *Tyrp1* and *Tyr*. This suggests that the requirement for SOX10 in the transcriptional regulation of these genes extends beyond activation of MITF expression.

#### SOX10 and BRG1 promote chromatin accessibility at common sites in the regulatory regions of co-regulated genes

To determine whether SOX10 and BRG1 are both required to promote chromatin accessibility at SOX10 binding sites in the distal enhancers of *Dct*, *Tyrp1* and *Tyr*, we transfected undifferentiated Melb-a cells with the respective siRNAs for 48 h, then shifted the cells to differentiation medium and performed FAIRE (Figure 8A–C). SOX10 depletion reduced chromatin accessibility at both the distal and proximal regulatory regions of *Dct* and the distal enhancer of *Tyrp1* to levels that were significantly below what was observed in undifferentiated Melb-a cells and reduced chromatin accessibility at proximal promoters as well as the *Tyr*

distal enhancer to levels significantly lower than in control differentiated cells. Since SOX10 regulates MITF expression and the proximal promoters have M boxes while the distal regions have E boxes that potentially bind MITF, we knocked down MITF to determine if the changes in accessibility that were observed in SOX10 knockdown cells might be indirectly due to loss of MITF. Depletion of MITF reduced chromatin accessibility at both the distal and proximal regulatory regions to levels that were significantly below those in control differentiated cells, bringing levels down to the levels in undifferentiated cells. Importantly, chromatin accessibility at the *Dct* and *Tyrp1* distal enhancers was significantly lower in SOX10 depleted cells than in MITF depleted cells. Knockdown of BRG1 also decreased accessibility at both the distal and proximal regions of *Dct*, *Tyrp1* and *Tyr* while knockdown of BRM slightly reduced chromatin accessibility at the distal and proximal promoters of *Tyrp1* and *Tyr* but had no effect on either region of *Dct*. Importantly, depletion of BRG1 resulted in reduced chromatin accessibility at all regulatory regions examined compared to depletion of BRM. These data suggest that SOX10 likely has a role in regulating chromatin structure at distal enhancers of some melanocyte-specific genes that extends beyond its role in regulating MITF expression and that BRG1 is the primary SWI/SNF ATPase that regulates chromatin accessibility at these sites.

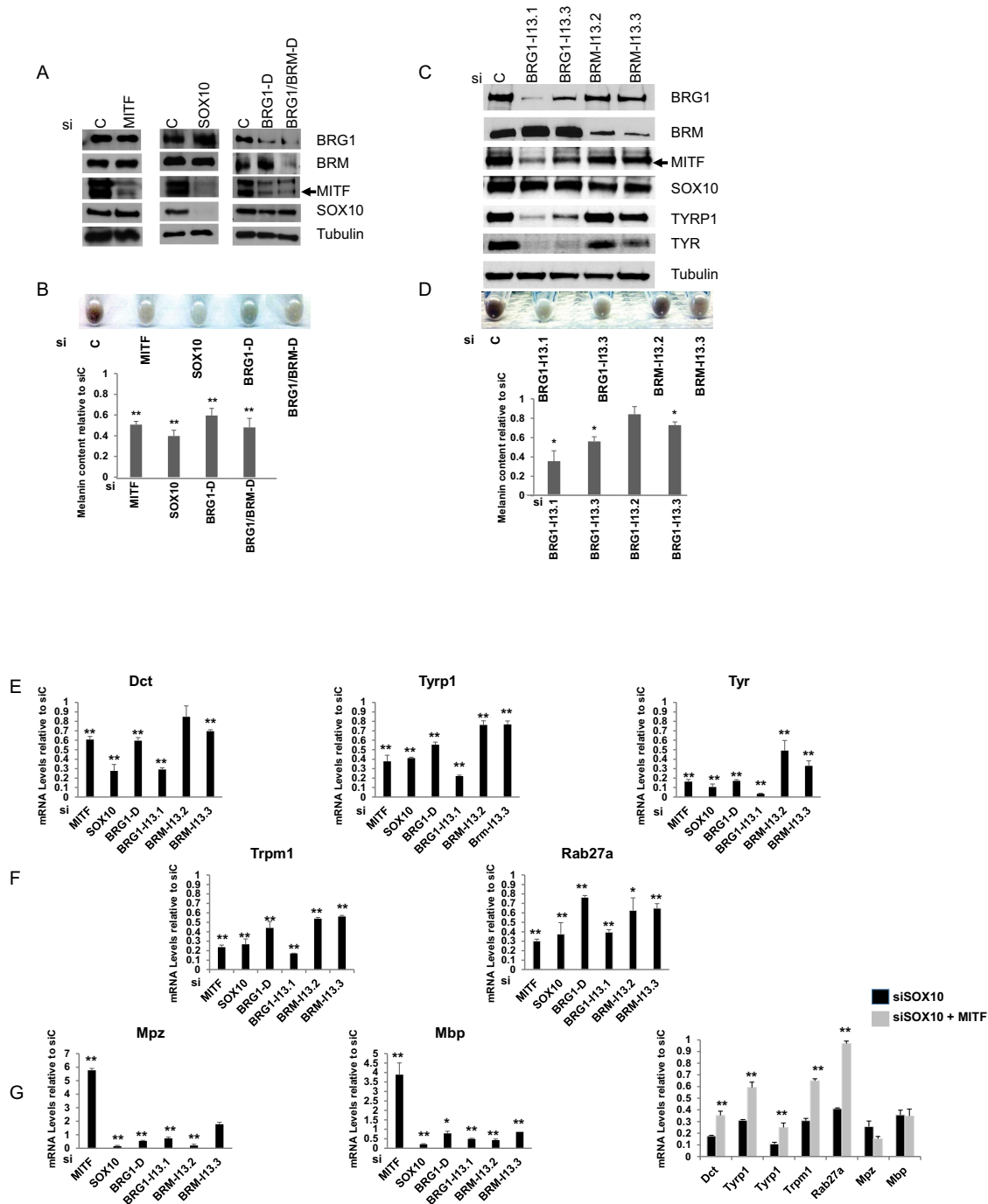


**Figure 7.** SOX10 and BRG1 are required for melanocyte differentiation. Undifferentiated Melb-a cells were transfected with the indicated siRNAs for 48 hours. The medium was then replaced by differentiation medium and cells were cultured for an additional 48 h. (A) Melb-a cells were subjected to Western blotting with antibodies to BRG1, BRM, MITF and SOX10. Tubulin was used as a loading control. (B) Melb-a cells transfected with the indicated siRNAs were pelleted and photographed. Cells were counted, and an equal number were subjected to the melanin assay. Each of the siRNAs resulted in a significant reduction in melanin relative to the siC. (C) Melb-a cells transfected with siRNAs that uniquely target BRG1 or BRM were subjected to Western blotting as in (A). Protein extracts were also evaluated for TYRP1 and TYR expression. (D) Melb-a cells transfected with siRNAs that uniquely target BRG1 or BRM were pelleted, photographed and subjected to the melanin assay as in (B). (E–G) RNA was isolated from siC, siMITF, siSOX10, siBRG1-D, siBRM-H13.1, siBRM-H13.2 and siBRM-H13.3 transfected Melb-a cells, reversed transcribed and quantified by qRT-PCR. The CT value for each gene was normalized to *Rpl7*. (E) Melanogenic enzyme gene expression. (F) Expression of genes associated with melanocyte differentiation. (G) Expression of myelin genes. The data are the average of at least two independent experiments performed in triplicate. Standard error bars and statistical significance compared to siC are shown (\*\* $P < 0.01$ , \* $P < 0.05$ , Student's *t* test). (H) Melb-a cells were co-transfected with siSOX10 and CMV-MITF. RNA was isolated from siC, siSOX10, and siSOX10/CMV-MITF transfected Melb-a cells, reversed transcribed and quantified by qRT-PCR. The CT values for each gene were normalized to *Rpl7* and are presented relative to values obtained with siC transfected cells. The data are the average of at least two independent experiments performed in triplicate. Standard error bars are shown. Stars indicate statistical difference between the MITF rescued siSOX10 cells compared to siSOX10 (\*\* $P < 0.01$ , \* $P < 0.05$ ).

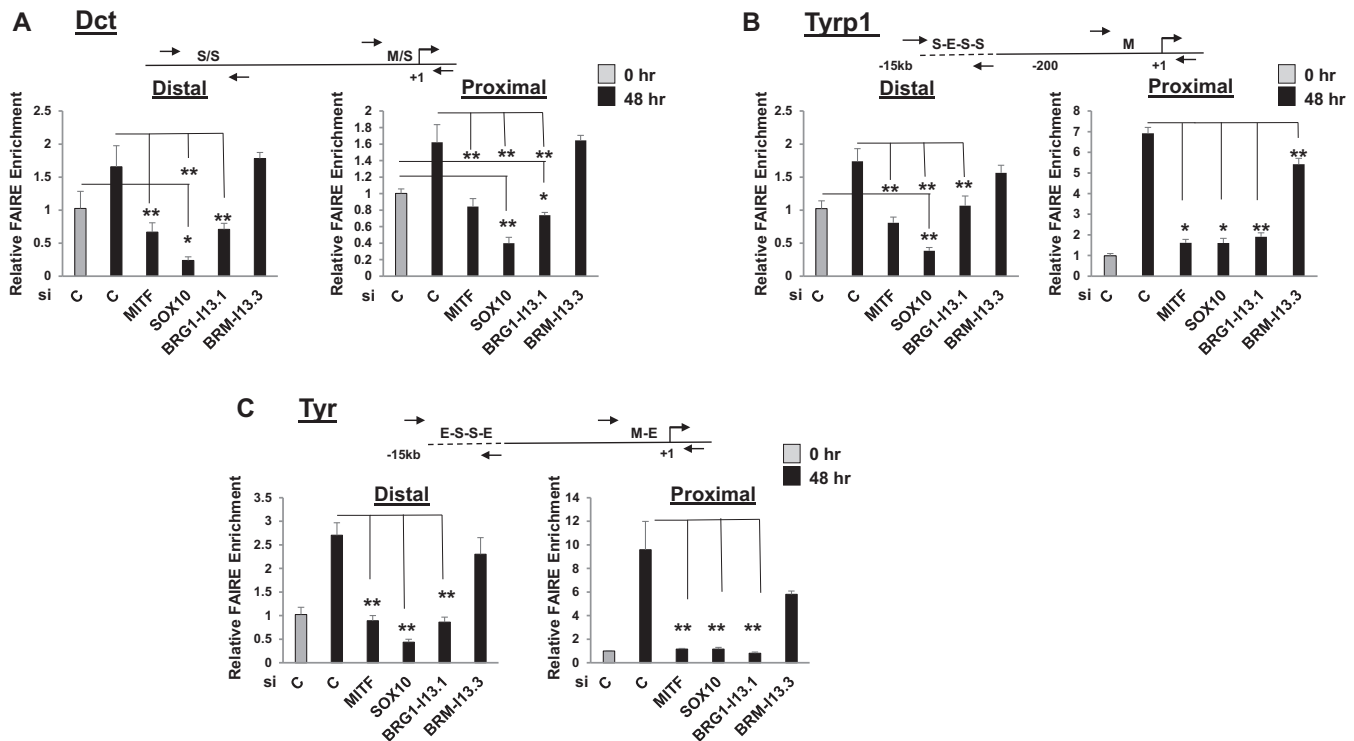


**Figure 8.** Knockdown of SOX10, MITF, or BRG1/BRM reduces chromatin accessibility at distal and proximal control regions of the melanogenic enzyme genes. (A–C). Undifferentiated Melb-a cells were transfected with siC, siMITF, siSOX10, siBRG1-I3.1 or siBRM13.3 for 48 h. The medium was then replaced by differentiation medium and cells were cultured for an additional 48 h. One set of cells was processed for FAIRE prior to differentiation (siC-undifferentiated). Cells were cross-linked and subjected to FAIRE analysis. Enrichment was quantified by qPCR by normalizing to an input (UnFAIRE) control for each primer set and to the *Scn2a1* region as a negative control. The data are the average of at least two independent experiments performed in triplicate. Standard error bars and statistical significance compared to siC undifferentiated (0hr) and differentiated (48 h) cells are shown (\*\* $P < 0.01$ , \* $P < 0.05$ , ANOVA).

### SOX10 physically interacts with BRG1 and recruits BRG1 to the *Tyrp1* enhancer in Melb-a cells

We performed co-immunoprecipitations to detect physical interactions between SOX10 and BRG1 in Melb-a cells. Using an antibody to pull down SOX10, we detected SOX10-BRG1 as well as SOX10-BRM complexes in both undifferentiated and differentiated Melb-a cells (Figure 9A, left). We also probed for the BAF60A subunit of the SWI/SNF complex which was previously shown to interact directly with SOX10 and promote BRG1 recruitment to Schwann cell-specific loci (14). As in Schwann cells, we detected a stronger interaction between SOX10 and BAF60A compared to a different subunit, BAF60B. This is consistent with the previous study that BAF60A mediates SOX10-SWI/SNF interactions and suggests that BRG1/BRM interact indirectly with SOX10 in melanocytes. Reciprocal co-immunoprecipitations using antibodies to BRG1 or BRM confirmed that SOX10 interacts with both BRG1 and BRM. We also probed for MITF and found that although BRG1-MITF as well as BRM-MITF complexes can be detected in undifferentiated cells, there is an increase in these complexes upon differentiation when MITF levels are higher (Figure 9A, right). These results show that SOX10 interacts with SWI/SNF complexes in both undifferentiated melanoblasts and in differentiated melanocytes and may facilitate SWI/SNF recruitment to distal regulatory regions

of melanogenic enzyme genes where SOX10 has a more pronounced role in chromatin remodeling.

Since chromatin at distal enhancers was found to be accessible in both undifferentiated and differentiated Melb-a cells and to be highly affected by knockdown of SOX10 but less so by MITF knockdown, we hypothesized that SOX10 recruits BRG1 to this site in order to remodel chromatin. The *Tyrp1* proximal region contains an M box which is the consensus binding site for MITF, and the distal region contains E boxes that potentially bind MITF. We found that there was little enrichment of MITF at either of these sites in undifferentiated Melb-a cells and that MITF became associated with both these sites 12 h after differentiation but that enrichment of MITF at the proximal region was higher than at the distal region (Figure 9B). SOX10 was constitutively enriched at the *Tyrp1* distal region in both undifferentiated and differentiated cells while a small but significant level of SOX10 enrichment occurred at the proximal region beginning 12 h after differentiation (Figure 9C). The significance of SOX10 enrichment at the proximal promoter regions is not clear since this region does not contain SOX10 binding sites. It may reflect non-specific binding which has been demonstrated by many transcription factors, including the SOX family member, SOX2, or it may reflect long range promoter-enhancer interactions, brought about by chromatin looping (70–72). Like SOX10, BRG1

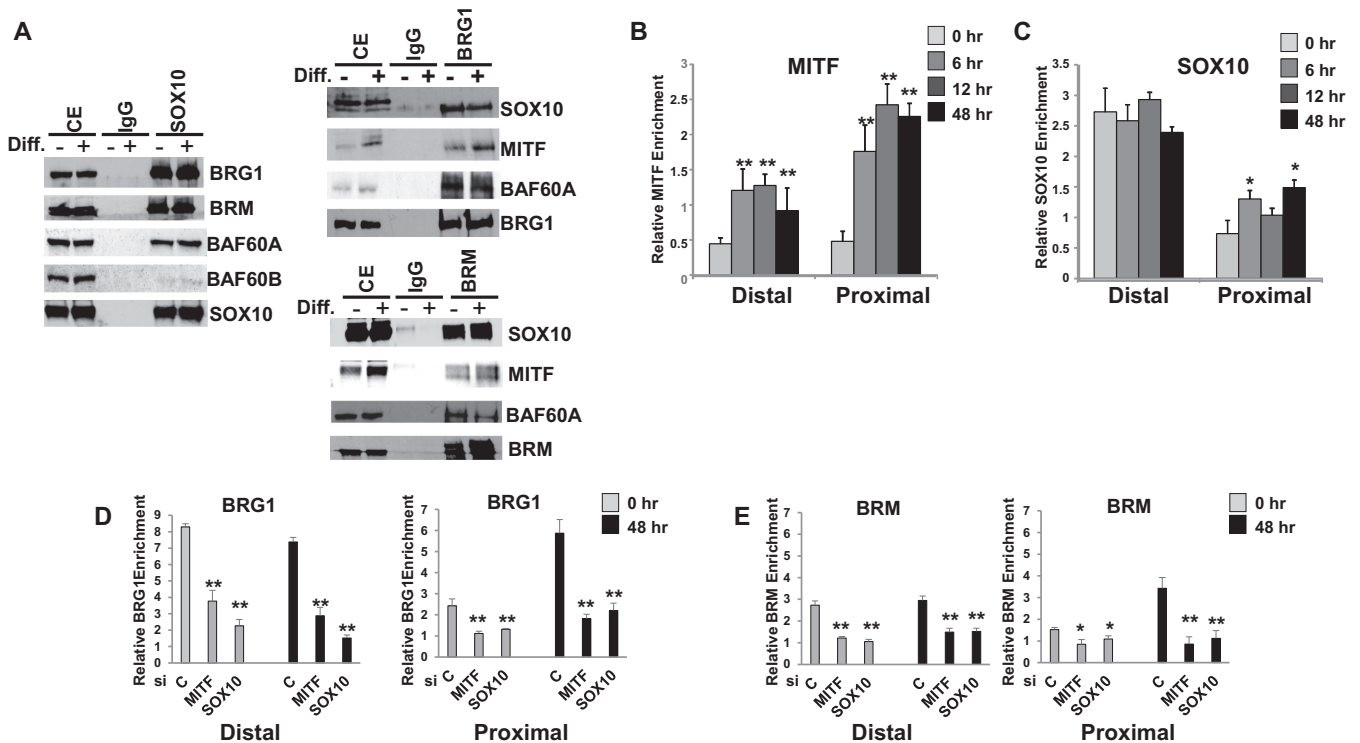


**Figure 9.** SOX10 physically interacts with BRG1 and recruits BRG1 to a melanocyte-specific enhancer in Melb-a cells. (A) Growing Melb-a cells or cells that had been differentiated for 18 h and either immunoprecipitated with an irrelevant antibody (IgG) or with an antibody to SOX10 (left), antiserum to BRG1 (top, right), or BRM (bottom, right). Cell extract (CE) or the immunoprecipitated material was run on an SDS-polyacrylamide gel and blotted with the indicated antibodies. (B) Chromatin immunoprecipitations (ChIPs) were performed with an antibody to MITF or control IgG. Enrichment of the *Tyrp1* distal and proximal regions was quantified by qPCR by normalizing to the IgG control for each primer set and to the *Scn2a1* region as a negative control region. The data are the average of at least two independent experiments performed in triplicate. Standard error bars and statistical significance compared to undifferentiated cells (0 h) are shown (\*\* $P < 0.01$ , \* $P < 0.05$ , Student's *t* test). (C) ChIP was performed and analyzed as in B using an antibody to SOX10 or control IgG. (D–E) Undifferentiated Melb-a cells were transfected with a control siRNA or siRNAs targeting MITF or SOX10 for 48 h. The medium was then replaced by differentiation medium and cells were cultured for an additional 48 h. (D) ChIP was performed and analyzed as in B using an antibody to BRG1 or as a control to IgG. (E) ChIP was performed and analyzed as in B using an antibody to BRM or as a control to IgG. The data are the average of at least two independent experiments performed in triplicate. Standard error bars and statistical significance compared to siC undifferentiated (0 h) and differentiated (48 h) cells are shown (\*\* $P < 0.01$ , \* $P < 0.05$ , ANOVA).

was found to be constitutively associated with the *Tyrp1* distal enhancer in both undifferentiated and differentiated Melb-a cells while recruitment to the *Tyrp1* proximal promoter increased during differentiation (Figure 9D). BRG1 recruitment to both these regions was decreased by depletion of either MITF or SOX10, with SOX10 depletion having a slightly greater effect on BRG1 recruitment to the distal enhancer than MITF depletion (Figure 9D). BRM also constitutively occupied the *Tyrp1* distal enhancer in both undifferentiated and differentiated cells, while recruitment to the proximal promoter increased upon differentiation and in an MITF- and SOX10-dependent manner. However, enrichment of BRM at the distal enhancer was substantially less than that of BRG1 (Figure 9E). In combination, these data suggest SOX10 facilitates recruitment of BRG1 to distal enhancers. Thus, BRG1 is a SOX10 co-activator, required to establish the melanocyte lineage and promote expression of genes important for melanocyte function.

## DISCUSSION

SOX10 interacts with a diverse set of transcriptional regulators to promote development of multiple cell lineages

and is essential for the survival and differentiation of neural crest-derived melanocytes and Schwann cells (7,8). As 'architectural transcription factors,' SOX proteins were originally thought exert their effects on transcription by virtue of their ability to bend DNA (73). However, activation of transcription by SOX10 has recently been associated with recruitment of chromatin remodeling enzymes to regulatory regions (14,15). *SOX10* was found to genetically and functionally interact with *Smarca4*, the gene encoding the BRG1 component of the SWI/SNF chromatin remodeling complex, to activate Schwann cell-specific gene expression at multiple steps in Schwann cell differentiation (14,15). BRG1-deficient mice exhibit Schwann cell defects strikingly similar to those seen in SOX10-deficient mice and these defects are exacerbated by additional heterozygous loss of one *SOX10* allele in BRG1-deficient mice. Our studies reveal that SOX10 also interacts genetically and functionally with BRG1 to promote melanocyte development. Utilizing an ENU-based mutagenesis screen, we found that heterozygous mutations in *Smarca4* exacerbate the spotting phenotype exhibited by *SOX10* haploinsufficient mice, resulting in severe hypopigmentation. This is strong evidence that SOX10 and BRG1 act together in the melanocyte lin-

age. In contrast, a genetic interaction between SOX10 and BRG1 was not observed during oligodendrocyte differentiation, despite a requirement for both SOX10 and BRG1 in this process (74). Instead, the requirement for BRG1 in oligodendrocyte differentiation may occur at a stage prior to when SOX10 is required. Thus, the observed interactions between SOX10 and BRG1 in melanocytes and Schwann cells may not be essential for differentiation of all cell types that express these proteins.

To confirm that disruption of BRG1 function was responsible for the observed hypopigmentation phenotype, we deleted *Smarca4* using a SOX10-Cre construct (33,34). Conditional deletion of *Smarca4* resulted in a striking loss of cranial and trunk melanoblasts (Figure 2). The observed loss of melanocytes is consistent with a previous study that utilized a *Tyr-Cre* construct to delete *Smarca4* (29), and confirms that BRG1 is required to establish the melanocyte lineage *in vivo*. It was previously unclear what happens to the melanocyte lineage when BRG1 is deleted. We now show that loss of BRG1 does not result in trans-differentiation to other neural crest lineages. Therefore, it is likely that loss of BRG1, like SOX10 and MITF, compromises melanoblast survival during embryonic development.

These results suggest that the alternative SWI/SNF ATPase, BRM, cannot compensate for the loss of BRG1 in the embryonic development of the melanocyte lineage. An absolute requirement for BRG1 and lack of compensation by BRM has been demonstrated in several other lineages including muscle (14,75–77). Indeed, our *in vitro* studies confirm that knockdown of BRG1 has a more profound effect on pigmentation, melanocyte-specific gene expression, and chromatin remodeling at several melanocyte-specific loci, than knockdown of the alternative ATPase, BRM. However, our data also show that BRM can interact with both SOX10 and MITF and be recruited to the regulatory regions of melanocyte-specific genes. It was previously shown that although BRM cannot compensate for BRG1 loss during embryonic development of vascular endothelial cells, BRM can compensate for BRG1 in maintaining these cells in the adult mouse heart (78). BRM null mice also display defects in muscle regeneration and BRM was found to be distinctly required for cell cycle arrest and late muscle specific gene expression (79). Our observations as well as other reports that associated BRM with highly differentiated cells (80) as well as melanocyte senescence (81) suggest that although BRM cannot compensate for BRG1 in early stages of melanocyte development, BRM may be important at later stages of melanocyte development or for melanocyte maintenance.

We found that SOX10 and BRG1 physically and functionally interact to promote melanocyte differentiation in cultured cells. The requirement for BRG1 in the melanocyte lineage has previously been attributed primarily to physical and functional interactions with MITF, which serve to recruit BRG1 to target genes involved in melanocyte differentiation, proliferation, and survival (28–29,41). However, BRG1 had also been reported to regulate MITF expression, to promote melanoma survival through MITF independent mechanisms, and to co-occupy SOX10 binding sites in melanoma cells (29,68,82). Establishing a functional interaction between SOX10 and BRG1 in melanocytes and

melanoma cells has been complicated because melanocyte genes are co-regulated by SOX10 and MITF, including MITF itself. Therefore, knockdown of SOX10 results in depletion of MITF, which then abrogates BRG1 recruitment. Our findings suggests that SOX10 facilitates recruitment of BRG1 to the *Tyrp1* distal enhancer. We found that SOX10 physically interacts with BRG1 in undifferentiated melanoblasts that express very low levels of MITF and that exhibit constitutively open chromatin structure at distal enhancers containing SOX10 binding sites. Furthermore, the timing of SOX10 and BRG1 binding to the *Tyrp1* distal enhancer coincide in undifferentiated melanoblasts, occurring when MITF binding to this region is very low. However, both SOX10 and MITF depletion compromised BRG1 recruitment to the *Tyrp1* distal enhancer, suggesting that SOX10 and MITF cooperate to recruit BRG1. In combination, these data suggest that in melanocyte precursors, SOX10 marks some melanocyte genes for later activation by MITF in part by recruiting BRG1 to distal enhancers.

In summary, we provide evidence that BRG1 is required for establishment of the melanocyte lineage *in vivo* and closely correlate this function with the role of SOX10 during melanocyte development. Our *in vitro* studies show that BRG1 is also required for melanin synthesis during melanocyte differentiation.

## SUPPLEMENTARY DATA

Supplementary Data are available at NAR Online.

## ACKNOWLEDGEMENTS

The authors would like to thank Laura Baxter for critical reading of the manuscript.

## FUNDING

National Institute of Arthritis and Musculoskeletal and Skin Diseases (NIAMS) [R01(ARO59379) to I.L.D.]; Deutsche Forschungsgemeinschaft (DFG) [We1326/8 to M.W.]; Wellcome Trust [078327 to D.C.B.]. Funding for open access charge: University of Toledo.

*Conflict of interest statement.* None declared.

## REFERENCES

- Bolande,R.P. (1997) Neurocristopathy: its growth and development in 20 years. *Pediatr. Pathol. Lab. Med.*, **17**, 1–25.
- Bondurand,N., Dastot-Le Moal,F., Stanchina,L., Collot,N., Baral,V., Marlin,S., Attie-Bitach,T., Giurgea,I., Skopinski,L., Reardon,W. *et al.* (2007) Deletions at the SOX10 gene locus cause Waardenburg syndrome types 2 and 4. *Am. J. Hum. Genet.*, **81**, 1169–1185.
- Pingault,V., Bondurand,N., Kuhlbrodt,K., Goerich,D.E., Prehu,M.O., Puliti,A., Herbarth,B., Hermans-Borgmeyer,I., Legius,E., Matthijs,G. *et al.* (1998) SOX10 mutations in patients with Waardenburg-Hirschsprung disease. *Nat. Genet.*, **18**, 171–173.
- Baldwin,C.T., Hoth,C.F., Amos,J.A., da-Silva,E.O. and Milunsky,A. (1992) An exonic mutation in the HuP2 paired domain gene causes Waardenburg's syndrome. *Nature*, **355**, 637–638.
- Tassabehji,M., Read,A.P., Newton,V.E., Harris,R., Balling,R., Gruss,P. and Strachan,T. (1992) Waardenburg's syndrome patients have mutations in the human homologue of the Pax-3 paired box gene. *Nature*, **355**, 635–636.

6. Tassabehji, M., Newton, V.E. and Read, A.P. (1994) Waardenburg syndrome type 2 caused by mutations in the human microphthalmia (MITF) gene. *Nat. Genet.*, **8**, 251–255.
7. Mollaaghababa, R. and Pavan, W.J. (2003) The importance of having your SOX on: role of SOX10 in the development of neural crest-derived melanocytes and glia. *Oncogene*, **22**, 3024–3034.
8. Wegner, M. (2005) Secrets to a healthy Sox life: lessons for melanocytes. *Pigment Cell Res.*, **18**, 74–85.
9. Jones, E.A., Jang, S.W., Mager, G.M., Chang, L.W., Srinivasan, R., Gokey, N.G., Ward, R.M., Nagarajan, R. and Svaren, J. (2007) Interactions of Sox10 and Egr2 in myelin gene regulation. *Neuron Glia Biol.*, **3**, 377–387.
10. LeBlanc, S.E., Ward, R.M. and Svaren, J. (2007) Neuropathy-associated Egr2 mutants disrupt cooperative activation of myelin protein zero by Egr2 and Sox10. *Mol. Cell Biol.*, **27**, 3521–3529.
11. Wei, Q., Miskimins, W.K. and Miskimins, R. (2004) Sox10 acts as a tissue-specific transcription factor enhancing activation of the myelin basic protein gene promoter by p27Kip1 and Sp1. *J. Neurosci. Res.*, **78**, 796–802.
12. Jagalur, N.B., Ghazvini, M., Mandemakers, W., Driegen, S., Maas, A., Jones, E.A., Jaegle, M., Grosveld, F., Svaren, J. and Meijer, D. (2011) Functional dissection of the Oct6 Schwann cell enhancer reveals an essential role for dimeric Sox10 binding. *J. Neurosci.*, **31**, 8585–8594.
13. Ghislain, J. and Charnay, P. (2006) Control of myelination in Schwann cells: a Krox20 cis-regulatory element integrates Oct6, Brn2 and Sox10 activities. *EMBO Rep.*, **7**, 52–58.
14. Weider, M., Kuspert, M., Bischof, M., Vogl, M.R., Hornig, J., Loy, K., Kosian, T., Muller, J., Hillgartner, S., Tamm, E.R. *et al.* (2012) Chromatin-remodeling factor Brg1 is required for Schwann cell differentiation and myelination. *Dev. Cell*, **23**, 193–201.
15. Marathe, H.G., Mehta, G., Zhang, X., Datar, I., Mehrotra, A., Yeung, K.C. and de la Serna, I.L. (2013) SWI/SNF Enzymes Promote SOX10-Mediated Activation of Myelin Gene Expression. *PLoS ONE*, **8**, e69037.
16. Imbalzano, A.N. (1998) Energy-dependent chromatin remodelers: complex complexes and their components. *Crit. Rev. Eukaryot. Gene Expr.*, **8**, 225–255.
17. Zhou, C.Y., Johnson, S.L., Gamarra, N.I. and Narlikar, G.J. (2016) Mechanisms of ATP-dependent chromatin remodeling motors. *Annu. Rev. Biophys.*, **45**, 153–181.
18. Imbalzano, A.N., Kwon, H., Green, M.R. and Kingston, R.E. (1994) Facilitated binding of TATA-binding protein to nucleosomal DNA. *Nature*, **370**, 481–485.
19. Kwon, H., Imbalzano, A.N., Khavari, P.A., Kingston, R.E. and Green, M.R. (1994) Nucleosome disruption and enhancement of activator binding by a human SWI/SNF complex. *Nature*, **370**, 477–481.
20. Vinod Saladi, S., Marathe, H. and de la Serna, I.L. (2010) SWITching on the transcriptional circuitry in melanoma. *Epigenetics*, **5**, 469–475.
21. Kowenz-Leutz, E. and Leutz, A. (1999) A C/EBP beta isoform recruits the SWI/SNF complex to activate myeloid genes. *Mol. Cell*, **4**, 735–743.
22. Pedersen, T.A., Kowenz-Leutz, E., Leutz, A. and Nerlov, C. (2001) Cooperation between C/EBPalpha TBP/TFIIB and SWI/SNF recruiting domains is required for adipocyte differentiation. *Genes Dev.*, **15**, 3208–3216.
23. Salma, N., Xiao, H., Mueller, E. and Imbalzano, A.N. (2004) Temporal recruitment of transcription factors and SWI/SNF chromatin-remodeling enzymes during adipogenic induction of the peroxisome proliferator-activated receptor gamma nuclear hormone receptor. *Mol. Cell Biol.*, **24**, 4651–4663.
24. de la Serna, I.L., Ohkawa, Y., Berkes, C.A., Bergstrom, D.A., Dacwag, C.S., Tapscott, S.J. and Imbalzano, A.N. (2005) MyoD targets chromatin remodeling complexes to the myogenin locus prior to forming a stable DNA-bound complex. *Mol. Cell Biol.*, **25**, 3997–4009.
25. Simone, C., Forcales, S.V., Hill, D.A., Imbalzano, A.N., Latella, L. and Puri, P.L. (2004) p38 pathway targets SWI-SNF chromatin-remodeling complex to muscle-specific loci. *Nat. Genet.*, **36**, 738–743.
26. Seo, S., Richardson, G.A. and Kroll, K.L. (2005) The SWI/SNF chromatin remodeling protein Brg1 is required for vertebrate neurogenesis and mediates transactivation of Ngn and NeuroD. *Development*, **132**, 105–115.
27. de la Serna, I.L., Ohkawa, Y., Higashi, C., Dutta, C., Osias, J., Kommajosyula, N., Tachibana, T. and Imbalzano, A.N. (2006) The microphthalmia-associated transcription factor requires SWI/SNF enzymes to activate melanocyte-specific genes. *J. Biol. Chem.*, **281**, 20233–20241.
28. Keenen, B., Qi, H., Saladi, S.V., Yeung, M. and de la Serna, I.L. (2010) Heterogeneous SWI/SNF chromatin remodeling complexes promote expression of microphthalmia-associated transcription factor target genes in melanoma. *Oncogene*, **29**, 81–92.
29. Laurette, P., Strub, T., Koludrovic, D., Keime, C., Le Gras, S., Seberg, H., Van Otterloo, E., Imrichova, H., Siddaway, R., Aerts, S. *et al.* (2015) Transcription factor MITF and remodeler BRG1 define chromatin organisation at regulatory elements in melanoma cells. *eLife*, **4**.
30. Saladi, S.V. and de la Serna, I.L. (2010) ATP dependent chromatin remodeling enzymes in embryonic stem cells. *Stem Cell Rev.*, **6**, 62–73.
31. Bultman, S., Gebuhr, T., Yee, D., La Mantia, C., Nicholson, J., Gilliam, A., Randazzo, F., Metzger, D., Chambon, P., Crabtree, G. *et al.* (2000) A Brg1 null mutation in the mouse reveals functional differences among mammalian SWI/SNF complexes. *Mol. Cell*, **6**, 1287–1295.
32. Matera, I., Watkins-Chow, D.E., Loftus, S.K., Hou, L., Incao, A., Silver, D.L., Rivas, C., Elliott, E.C., Baxter, L.L. and Pavan, W.J. (2008) A sensitized mutagenesis screen identifies Gli3 as a modifier of Sox10 neurocristopathy. *Hum. Mol. Genet.*, **17**, 2118–2131.
33. Matsuoka, T., Ahlberg, P.E., Kessaris, N., Iannarelli, P., Dennehy, U., Richardson, W.D., McMahon, A.P. and Koentges, G. (2005) Neural crest origins of the neck and shoulder. *Nature*, **436**, 347–355.
34. Sumi-Ichinose, C., Ichinose, H., Metzger, D. and Chambon, P. (1997) SNF2beta-BRG1 is essential for the viability of F9 murine embryonal carcinoma cells. *Mol. Cell Biol.*, **17**, 5976–5986.
35. Witmer, P.D., Doheny, K.F., Adams, M.K., Boehm, C.D., Dizon, J.S., Goldstein, J.L., Templeton, T.M., Wheaton, A.M., Dong, P.N., Pugh, E.W. *et al.* (2003) The development of a highly informative mouse Simple Sequence Length Polymorphism (SSLP) marker set and construction of a mouse family tree using parsimony analysis. *Genome Res.*, **13**, 485–491.
36. Stolt, C.C., Lommes, P., Hillgartner, S. and Wegner, M. (2008) The transcription factor Sox5 modulates Sox10 function during melanocyte development. *Nucleic Acids Res.*, **36**, 5427–5440.
37. Maka, M., Stolt, C.C. and Wegner, M. (2005) Identification of Sox8 as a modifier gene in a mouse model of Hirschsprung disease reveals underlying molecular defect. *Dev. Biol.*, **277**, 155–169.
38. de la Serna, I.L., Carlson, K.A., Hill, D.A., Guidi, C.J., Stephenson, R.O., Sif, S., Kingston, R.E. and Imbalzano, A.N. (2000) Mammalian SWI-SNF complexes contribute to activation of the hsp70 gene. *Mol. Cell Biol.*, **20**, 2839–2851.
39. Sviderskaya, E.V., Hill, S.P., Balachandar, D., Barsh, G.S. and Bennett, D.C. (2001) Agouti signaling protein and other factors modulating differentiation and proliferation of immortal melanoblasts. *Dev. Dyn.*, **221**, 373–379.
40. Eller, M.S., Ostrom, K. and Gilchrist, B.A. (1996) DNA damage enhances melanogenesis. *Proc. Natl. Acad. Sci. U.S.A.*, **93**, 1087–1092.
41. Saladi, S.V., Wong, P.G., Trivedi, A.R., Marathe, H.G., Keenen, B., Aras, S., Liew, Z.Q., Setaluri, V. and de la Serna, I.L. (2013) BRG1 promotes survival of UV-irradiated melanoma cells by cooperating with MITF to activate the melanoma inhibitor of apoptosis gene. *Pigment Cell Melanoma Res.*, **26**, 377–391.
42. Carreira, S., Goodall, J., Aksan, I., La Rocca, S.A., Galibert, M.D., Denat, L., Larue, L. and Goding, C.R. (2005) Mitf cooperates with Rb1 and activates p21Cip1 expression to regulate cell cycle progression. *Nature*, **433**, 764–769.
43. Carreira, S., Goodall, J., Denat, L., Rodriguez, M., Nuciforo, P., Hoek, K.S., Testori, A., Larue, L. and Goding, C.R. (2006) Mitf regulation of Dia 1 controls melanoma proliferation and invasiveness. *Genes Dev.*, **20**, 3426–3439.
44. Bourseguin, J., Bonet, C., Renaud, E., Pandiani, C., Boncompagni, M., Giuliano, S., Pawlikowska, P., Karmous-Benailly, H., Ballotti, R., Rosselli, F. *et al.* (2016) FANCD2 functions as a critical factor downstream of MITF to maintain the proliferation and survival of melanoma cells. *Sci. Rep.*, **6**, 36539.



45. Kuspert, M., Weider, M., Muller, J., Hermans-Borgmeyer, I., Meijer, D. and Wegner, M. (2012) Desert hedgehog links transcription factor Sox10 to perineurial development. *J. Neurosci.*, **32**, 5472–5480.
46. Ramirez-Carrozzi, V.R., Nazarian, A.A., Li, C.C., Gore, S.L., Sridharan, R., Imbalzano, A.N. and Smale, S.T. (2006) Selective and antagonistic functions of SWI/SNF and Mi-2beta nucleosome remodeling complexes during an inflammatory response. *Genes Dev.*, **20**, 282–296.
47. Simon, J.M., Giresi, P.G., Davis, I.J. and Lieb, J.D. (2012) Using formaldehyde-assisted isolation of regulatory elements (FAIRE) to isolate active regulatory DNA. *Nat. Protoc.*, **7**, 256–267.
48. Giresi, P.G. and Lieb, J.D. Isolation of active regulatory elements from eukaryotic chromatin using FAIRE (Formaldehyde Assisted Isolation of Regulatory Elements). *Methods* (2009) **48** 233-9
49. Law, C. and Cheung, P. (2015) Expression of non-acetylatable H2A.Z in myoblast cells blocks myoblast differentiation through disruption of MyoD expression. *J. Biol. Chem.*, **290**, 13234–13249.
50. Lang, D., Lu, M.M., Huang, L., Engleka, K.A., Zhang, M., Chu, E.Y., Lipner, S., Skoultschi, A., Millar, S.E. and Epstein, J.A. (2005) Pax3 functions at a nodal point in melanocyte stem cell differentiation. *Nature*, **433**, 884–887.
51. Miller, A.J., Du, J., Rowan, S., Hershey, C.L., Widlund, H.R. and Fisher, D.E. (2004) Transcriptional regulation of the melanoma prognostic marker melastatin (TRPM1) by MITF in melanocytes and melanoma. *Cancer Res.*, **64**, 509–516.
52. Zhiqi, S., Soltani, M.H., Bhat, K.M., Sangha, N., Fang, D., Hunter, J.J. and Setaluri, V. (2004) Human melastatin 1 (TRPM1) is regulated by MITF and produces multiple polypeptide isoforms in melanocytes and melanoma. *Melanoma Res.*, **14**, 509–516.
53. Chiaverini, C., Beuret, L., Flori, E., Busca, R., Abbe, P., Bille, K., Bahadoran, P., Ortonne, J.P., Bertolotto, C. and Ballotti, R. (2008) Microphthalmia-associated transcription factor regulates RAB27A gene expression and controls melanosome transport. *J. Biol. Chem.*, **283**, 12635–12642.
54. Hoek, K.S., Schlegel, N.C., Eichhoff, O.M., Widmer, D.S., Praetorius, C., Einarsson, S.O., Valgeirsdottir, S., Bergsteinsdottir, K., Schepsky, A., Dummer, R. et al. (2008) Novel MITF targets identified using a two-step DNA microarray strategy. *Pigment Cell Melanoma Res.*, **21**, 665–676.
55. Strub, T., Giuliano, S., Ye, T., Bonet, C., Keime, C., Kobi, D., Le Gras, S., Cormont, M., Ballotti, R., Bertolotto, C. et al. (2011) Essential role of microphthalmia transcription factor for DNA replication, mitosis and genomic stability in melanoma. *Oncogene*, **30**, 2319–2332.
56. Serra, C., Palacios, D., Mozzetta, C., Forcales, S.V., Morante, I., Ripani, M., Jones, D.R., Du, K., Jhala, U.S., Simone, C. et al. (2007) Functional interdependence at the chromatin level between the MKK6/p38 and IGF1/PI3K/AKT pathways during muscle differentiation. *Mol. Cell*, **28**, 200–213.
57. Salma, N., Xiao, H. and Imbalzano, A.N. (2006) Temporal recruitment of CCAAT/enhancer-binding proteins to early and late adipogenic promoters in vivo. *J. Mol. Endocrinol.*, **36**, 139–151.
58. Xiao, H., Leblanc, S.E., Wu, Q., Konda, S., Salma, N., Marfella, C.G., Ohkawa, Y. and Imbalzano, A.N. (2011) Chromatin accessibility and transcription factor binding at the PPARgamma2 promoter during adipogenesis is protein kinase A-dependent. *J. Cell Physiol.*, **226**, 86–93.
59. Sviderskaya, E.V., Wakeling, W.F. and Bennett, D.C. (1995) A cloned, immortal line of murine melanoblasts inducible to differentiate to melanocytes. *Development*, **121**, 1547–1557.
60. Bennett, D.C. (1983) Differentiation in mouse melanoma cells: initial reversibility and an on-off stochastic model. *Cell*, **34**, 445–453.
61. Giresi, P.G., Kim, J., McDaniel, R.M., Iyer, V.R. and Lieb, J.D. (2007) FAIRE (Formaldehyde-Assisted Isolation of Regulatory Elements) isolates active regulatory elements from human chromatin. *Genome Res.*, **17**, 877–885.
62. Lowings, P., Yavuzer, U. and Goding, C.R. (1992) Positive and negative elements regulate a melanocyte-specific promoter. *Mol. Cell Biol.*, **12**, 3653–3662.
63. Ganss, R., Schutz, G. and Beermann, F. (1994) The mouse tyrosinase gene. Promoter modulation by positive and negative regulatory elements. *J. Biol. Chem.*, **269**, 29808–29816.
64. Murisier, F., Guichard, S. and Beermann, F. (2006) A conserved transcriptional enhancer that specifies Tyrp1 expression to melanocytes. *Dev. Biol.*, **298**, 644–655.
65. Murisier, F., Guichard, S. and Beermann, F. (2007) The tyrosinase enhancer is activated by Sox10 and Mitf in mouse melanocytes. *Pigment Cell Res.*, **20**, 173–184.
66. Yao, L., Berman, B.P. and Farnham, P.J. (2015) Demystifying the secret mission of enhancers: linking distal regulatory elements to target genes. *Crit. Rev. Biochem. Mol. Biol.*, **50**, 550–573.
67. Potterf, S.B., Furumura, M., Dunn, K.J., Arnheiter, H. and Pavan, W.J. (2000) Transcription factor hierarchy in Waardenburg syndrome: regulation of MITF expression by SOX10 and PAX3. *Hum. Genet.*, **107**, 1–6.
68. Vachtenheim, J., Ondrusova, L. and Borovansky, J. (2010) SWI/SNF chromatin remodeling complex is critical for the expression of microphthalmia-associated transcription factor in melanoma cells. *Biochem. Biophys. Res. Commun.*, **392**, 454–459.
69. Limpert, A.S., Bai, S., Narayan, M., Wu, J., Yoon, S.O., Carter, B.D. and Lu, Q.R. (2013) NF-kappaB forms a complex with the chromatin remodeler BRG1 to regulate Schwann cell differentiation. *J. Neurosci.*, **33**, 2388–2397.
70. Biggin, M.D. (2011) Animal transcription networks as highly connected, quantitative continua. *Dev. Cell*, **21**, 611–626.
71. Soufi, A., Garcia, M.F., Jaroszewicz, A., Osman, N., Pellegrini, M. and Zaret, K.S. (2015) Pioneer transcription factors target partial DNA motifs on nucleosomes to initiate reprogramming. *Cell*, **161**, 555–568.
72. LeBlanc, S.E., Wu, Q., Lamba, P., Sif, S. and Imbalzano, A.N. (2016) Promoter-enhancer looping at the PPARgamma2 locus during adipogenic differentiation requires the Prmt5 methyltransferase. *Nucleic Acids Res.*, **44**, 5133–5147.
73. Werner, M.H. and Burley, S.K. (1997) Architectural transcription factors: proteins that remodel DNA. *Cell*, **88**, 733–736.
74. Bischof, M., Weider, M., Kuspert, M., Nave, K.A. and Wegner, M. (2015) Brg1-dependent chromatin remodelling is not essentially required during oligodendroglial differentiation. *J. Neurosci.*, **35**, 21–35.
75. Lickert, H., Takeuchi, J.K., Von Both, I., Walls, J.R., McAuliffe, F., Adamson, S.L., Henkelman, R.M., Wrana, J.L., Rossant, J. and Bruneau, B.G. (2004) Baf60c is essential for function of BAF chromatin remodelling complexes in heart development. *Nature*, **432**, 107–112.
76. Griffin, C.T., Brennan, J. and Magnuson, T. (2008) The chromatin-remodeling enzyme BRG1 plays an essential role in primitive erythropoiesis and vascular development. *Development*, **135**, 493–500.
77. Griffin, C.T., Curtis, C.D., Davis, R.B., Muthukumar, V. and Magnuson, T. (2011) The chromatin-remodeling enzyme BRG1 modulates vascular Wnt signaling at two levels. *Proc. Natl. Acad. Sci. U.S.A.*, **108**, 2282–2287.
78. Willis, M.S., Homeister, J.W., Rosson, G.B., Annayev, Y., Holley, D., Holly, S.P., Madden, V.J., Godfrey, V., Parise, L.V. and Bultman, S.J. (2012) Functional redundancy of SWI/SNF catalytic subunits in maintaining vascular endothelial cells in the adult heart. *Circ. Res.*, **111**, e111–122.
79. Albini, S., Coutinho Toto, P., Dall’Agnese, A., Malecova, B., Cenciarelli, C., Felsani, A., Caruso, M., Bultman, S.J. and Puri, P.L. (2015) Brahma is required for cell cycle arrest and late muscle gene expression during skeletal myogenesis. *EMBO Rep.*, **16**, 1037–1050.
80. Reisman, D.N., Sciarrotta, J., Bouldin, T.W., Weissman, B.E. and Funkhouser, W.K. (2005) The expression of the SWI/SNF ATPase subunits BRG1 and BRM in normal human tissues. *Appl. Immunohistochem. Mol. Morphol.*, **13**, 66–74.
81. Bandyopadhyay, D., Curry, J.L., Lin, Q., Richards, H.W., Chen, D., Hornsby, P.J., Timchenko, N.A. and Medrano, E.E. (2007) Dynamic assembly of chromatin complexes during cellular senescence: implications for the growth arrest of human melanocytic nevi. *Aging Cell*, **6**, 577–591.
82. Ondrusova, L., Vachtenheim, J., Reda, J., Zakova, P. and Benkova, K. (2013) MITF-independent pro-survival role of BRG1-containing SWI/SNF complex in melanoma cells. *PLoS ONE*, **8**, e54110.